Journal of Asian Earth Sciences 137 (2017) 9–34

Contents lists available at ScienceDirect

Journal of Asian Earth Sciences

journal homepage: www.elsevier.com/locate/jseaes

The giant South China Mesozoic low-temperature metallogenic domain: Reviews and a new geodynamic model

Ruizhong Hu [a,*], Shanling Fu [a], Yong Huang [a], Mei-Fu Zhou [b], Shaohong Fu [a], Chenghai Zhao [a], Yuejun Wang [c], Xianwu Bi [a], Jiafei Xiao [a]

[a] State Key Laboratory of Ore Deposit Geochemistry, Institute of Geochemistry, Chinese Academy of Sciences, Guiyang 550081, China
[b] Department of Earth Sciences, The University of Hong Kong, Hong Kong, China
[c] School of Earth Science & Geological Engineering, Sun YatSen University, Guangzhou 510275, China

ARTICLE INFO

Article history:
Received 10 August 2016
Received in revised form 24 October 2016
Accepted 29 October 2016
Available online 15 November 2016

Keywords:
South China
Low-temperature mineralization
Indosinian orogeny
Yanshanian orogeny
Polymetallic mineral deposits

ABSTRACT

The South China Craton was formed by amalgamation of the Yangtze and Cathaysia Blocks during the Neoproterozoic. During the Mesozoic, voluminous granitic plutons and associated W-Sn polymetallic deposits were formed in the Cathaysia Block. The giant South China low-temperature metallogenic domain (LTMD) includes an area of ~500,000 km^2 in the Yangtze Block and is composed of the Chuan-Dian-Qian Pb-Zn, Youjiang Au-As-Sb-Hg and Xiangzhong Sb-Au metallogenic provinces. The Chuan-Dian-Qian Pb-Zn province contains numerous MVT Pb-Zn deposits, whereas the other two provinces are characterized by Carlin-type Au deposits and vein-type Sb, Hg and As deposits. These epigenetic deposits, which formed under low temperature conditions (~100–250 °C), are typically hosted in sedimentary rocks and are locally controlled by faults and fractures. The deposits formed dominantly at 200–230 Ma and 130–160 Ma, corresponding to Indosinian (Triassic) and Yanshanian (Jurassic to Cretaceous) orogenies, respectively. Indosinian mineralization is recognized in all three provinces, but Yanshanian mineralization occurred only in the Youjiang and Xiangzhong provinces. The Indosinian orogeny, which involved collision of the Indochina Block with the South China Craton, resulted in circulation of basinal brines that leached ore-forming elements from adjacent sedimentary strata to form the Chuan-Dian-Qian Pb-Zn province. Deep-seated granitic magmas generated during this orogeny caused extensive circulation of meteoric water that mobilized ore-forming elements from the sedimentary strata to form the Carlin-type Au deposits in the Youjiang province, and the Sb-Au deposits in the Xiangzhong province. The Indosinian orogeny was the key factor in establishing the metallogenic framework of the LTMD. It produced widespread mineralization in the three metallogenic provinces, each of which has unique features reflecting differences in the nature and composition of the basement rocks. The Yanshanian metallogeny was less important and overprinted the older ore deposits in the Youjiang and Xiangzhong provinces.

1. Introduction

Metallogenic domains are defined as huge regions that contain a large number of ore deposits. An extremely important group of low-temperature (generally below 200–250 °C), hydrothermal deposits, has been termed the South China low-temperature metallogenic domain (LTMD; Tu, 1998, 2002; Li, 1999). This domain extends over an area of ~500,000 km^2 in the southwestern part of the Yangtze Block and includes world-class Carlin-type gold deposits, vein-type Sb, Hg and As deposits and Mississippi Valley-type (MVT) Pb-Zn deposits (Hu et al., 2002; Su et al., 2008, 2009a, 2009b, 2012; Hu and Zhou, 2012; Peng et al., 2003b; Zhou et al., 2001; Zhou et al., 2013a, 2013b, 2013c; J.X. Zhou et al., 2014; M.F. Zhou et al., 2014; Zhou et al., 2015; Chen et al., 2015). The LTMD accounts for more than 50% of the Sb reserves of the world (Peng et al., 2003a, 2014a), and ~10% of the Au reserves (Su et al., 2016, in review) and 80% of the Hg reserves of China (Hua and Cui, 1996). A particular feature of this domain is its association of a variety of deposits including Carlin-type Au, Mississippi Valley-type Pb-Zn and important Sb, Hg and As deposits.

Extensive studies of the low-temperature ore deposits in South China started in the 1970s and have resulted in many discoveries

* Corresponding author.
E-mail address: huruizhong@vip.gyig.ac.cn (R.Z. Hu).

http://dx.doi.org/10.1016/j.jseaes.2016.10.016
1367-9120/

of different types of deposits. It is now widely accepted that the LTMD includes the Chuan-Dian-Qian Pb-Zn, Youjiang Au-As-Sb-Hg and Xiangzhong Sb-Au domains (Hu et al., 2015). These low-temperature (~100–250 °C) epigenetic deposits are typically hosted in deformed sedimentary rocks which have structural styles of fault-related folds (Zhou et al., 2001; Hu et al., 2002; Peng et al., 2003a; Chen et al., 2015). However, their origin and geodynamic environments have long been matters of debate. The debate is largely due to the lack of the age constraints on these deposits. Hu and Zhou (2012) and Mao et al. (2013) reviewed the Mesozoic metallogeny in South China, but these papers are mainly focused on granite-related, W-Sn polymetallic deposits in the Cathaysia Block.

In the past decade, abundant new data has become available and it is now clear that these deposits were mostly formed at 200–230 Ma and 130–160 Ma, corresponding to the Indosinian (Triassic) and Yanshanian (Jurassic to Cretaceous) orogenies, respectively. Thus, it is now timely to review the existing literature in order to generate a comprehensive genetic model. In this paper, we bring together all possible data and review currently existing models for the Mesozoic deposits in the LTMD. On the basis of this review, we propose a new geodynamic model to explain the formation of the LTMD.

2. Geological background

The South China Craton in the southeastern part of the Eurasian continent is made up of the Yangtze Block to the northwest and the Cathaysia Block to the southeast, which were amalgamated along the Jiangshao suture zone, which extends from Shaoxing in the northeast through the south of Changsha to the east of Nanning (Yao et al., 2016), at around 830 Ma (Zhao et al., 2011). In the Triassic, the South China Craton was welded together with the North China Craton to the north and the Indochina Block to the south (Faure and Ishida, 1990; M.F. Zhou et al., 2006; Wang et al., 2007a; Fig. 1).

The basement of the Yangtze Block is composed of late Archean metamorphic rocks in the north and younger, only weakly metamorphosed late Paleoproterozoic to Neoproterozoic rocks in the west and east, all of which were later intruded by widespread Neoproterozoic igneous rocks (Zhou et al., 2002; J.X. Zhou et al., 2014; M.F. Zhou et al., 2014). The sedimentary succession of the Yangtze Block consists mainly of Cambrian to Triassic marine sedimentary rocks and Jurassic, Cretaceous and Cenozoic continental sedimentary rocks (Yan et al., 2003).

The Cathaysia Block is characterized by widespread, 1.9–1.8-Ga sedimentary rocks and Neoproterozoic to Early Paleozoic metamorphic rocks (Yu et al., 2005). Due to an Early Paleozoic orogeny, Late Ordovician to Middle Devonian strata are absent but there are widespread granitic intrusions with ages ranging from 480 to 400 Ma (Yu et al., 2005).

An important Mesozoic event in the South China Craton was the formation of a large granite province and associated large-scale Mesozoic metallogeny in both the Yangtze and Cathaysia Blocks (Gilder et al., 1996; Chen and Jahn, 1998; Li, 2000; X.M. Zhou et al., 2006; Li and Li; 2007; Wang et al., 2007b; Zaw et al., 2007; Hu and Zhou, 2012; Mao et al., 2013). Indosinian magmatism

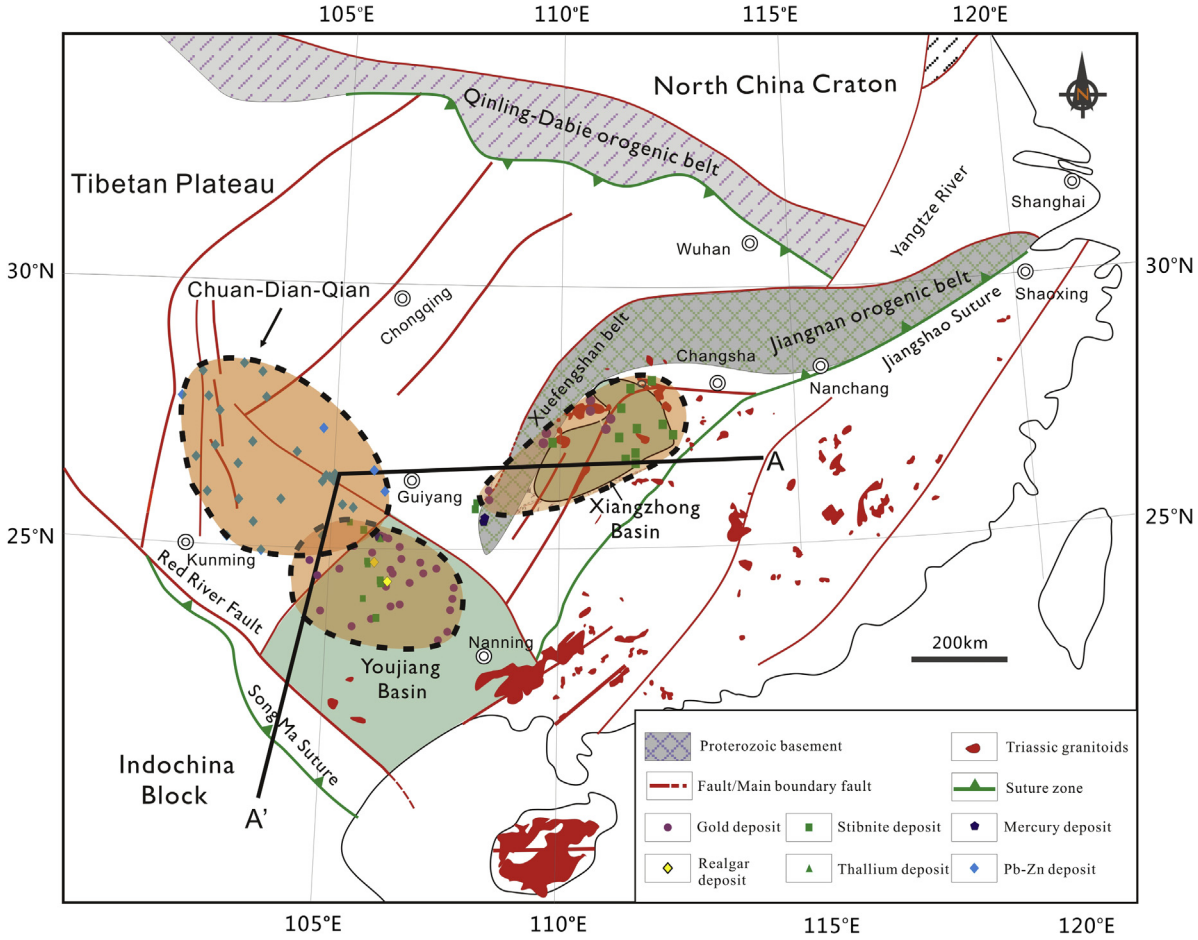

Fig. 1. A simplified geological map of the South China Craton and adjacent regions showing the structural framework and the distribution of low-temperature ore deposits in the Yangtze Block (modified from Hu et al., 2002; G.W. Zhang et al., 2013; Qiu et al., 2016; Yao et al., 2016).

produced voluminous granitic plutons in the South China Craton (e.g. Qiu et al., 2016; Wu et al., 2016), mainly in the Cathaysian Block and eastern part of the Yangtze Block, which range in age, from ca. 255 to 200 Ma (Wang et al., 2005, 2007a, 2007b; X.M. Zhou et al., 2006; C.H. Chen et al., 2011, 2015). The Indosinian magmatism has been related to westward subduction of the Paleo-Pacific plate underneath the eastern margin of the Eurasian continent (Cui and Li, 1983; Li and Li, 2007). The Indosinian deformation and magmatism may also have been due to collision between the Indochina Block and South China Craton in response to the closure of Paleotethys (Wang et al., 2005, 2007a, 2007b; X.M. Zhou et al., 2006; Lepvrier et al., 2004; C.H. Chen et al., 2011; Qiu et al., 2016).

The giant Yanshanian granitic province forms a swath >1000 km wide across the whole Cathaysia Block (Li and Li, 2007). These granitic rocks were formed mainly in the Jurassic to Cretaceous, notably at 160–150 Ma and 120–85 Ma, respectively (Mao et al., 2013; Yang et al., 2016; Chen et al., 2016). The formation of this province was probably related to the westward subduction of the Pacific oceanic lithosphere beneath the Eurasian continent (X.M. Zhou et al., 2006; Li and Li, 2007). The Yanshanian granitic intrusions are mostly distributed in the Cathaysia Block with some in the Yangtze Block (Hu and Zhou, 2012).

In the Cathaysia Block, numerous Mesozoic granitic intrusions host most of the world's W-Sn deposits (Hu and Zhou, 2012; Mao et al., 2013), but Mesozoic, low-temperature mineral deposits occur mostly in the Yangtze Block (Zhou et al., 2001; Hu et al., 2002; Su et al., 2008, 2009a, 2009b, 2012; Hu and Zhou, 2012; Peng et al., 2003b; Chen et al., 2015). The hydrothermal deposits, including Carlin-type gold deposits, MVT Pb-Zn deposits and vein-type Sb, Hg, As and Tl deposits, form a low-temperature metallogenic domain with an area of ~500,000 km^2 (Tu, 2002; Hu et al., 2002, 2015; Fig. 1), which includes the Chuan-Dian-Qian Pb-Zn, Youjiang Au-as-Sb-Hg and Xiangzhong Sb-Au metallogenic provinces (Fig. 1). Proven Sb, Au and Hg reserves in this province account for ~50% of the global Sb (Peng et al., 2003a, 2014a), and 10% and 80% of the Chinese Au and Hg, respectively (Su et al., 2016, in review; Hua and Cui, 1996). The province is also one of the main producers of Pb and Zn in China (C.Q. Zhang et al., 2005).

3. Chuan-Dian-Qian Pb-Zn metallogenic province

3.1. Regional geology

The Chuan-Dian-Qian Pb-Zn metallogenic province at the southwestern margin of the Yangtze Block (Fig. 1) hosts more than 400 Pb-Zn deposits (occurrences), making it one of the most important Pb-Zn mineralization areas in China (Fig. 2; J.X. Zhou et al., 2014; M.F. Zhou et al., 2014). In this region, the folded basement rocks include those of the Kangding, Dahongshan and Kunyang Groups, consisting of well-bedded greywackes, slates and carbonaceous to siliceous sedimentary rocks, which are tightly folded but only weakly metamorphosed. The widely distributed, shallow marine Paleozoic and Lower Mesozoic cover rocks include

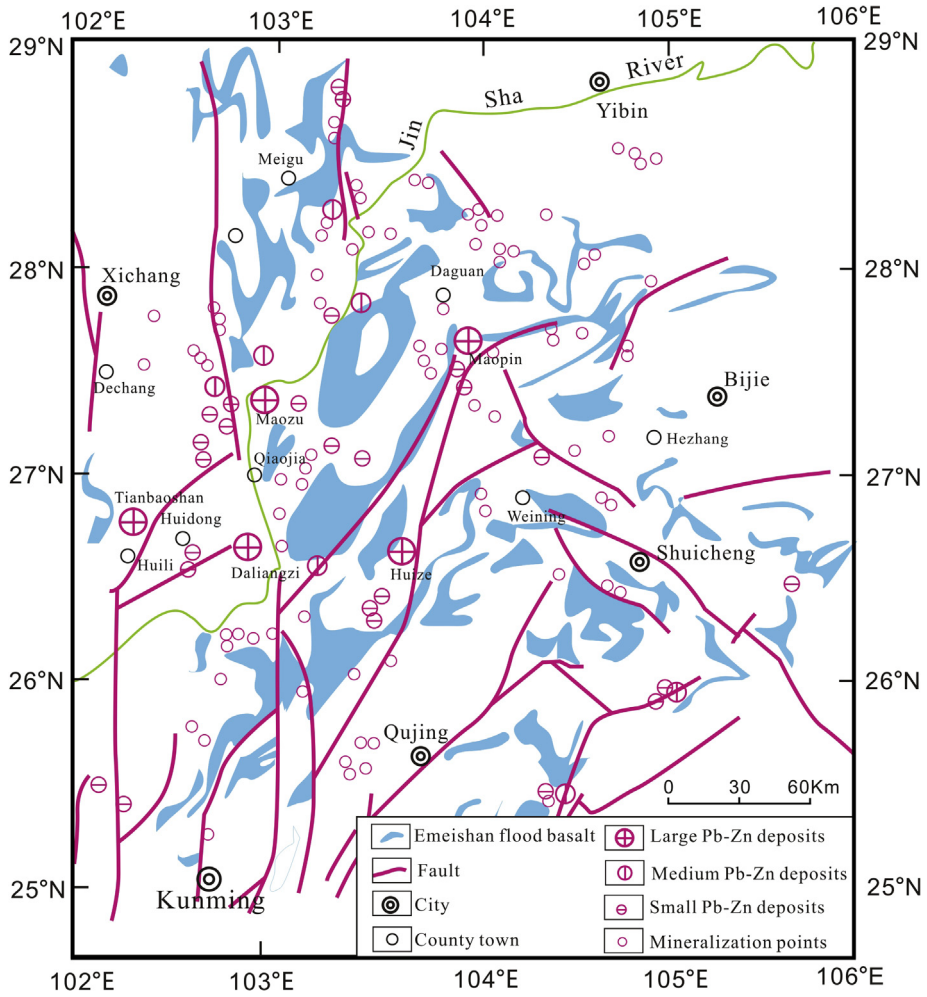

Fig. 2. A map showing the distribution of Pb-Zn deposits in the Chuan-Dian-Qian metallogenic province (modified from Zhou et al., 2013c).

Cambrian black shale, sandstone and limestone interbedded with dolostone, Ordovician sequences of thick-bedded limestone interlayered with dolostone and argillaceous siltstone, and Devonian to Permian limestone and dolostone interbedded with minor clastic rocks (Zhou et al., 2001, 2013b). Permian Emeishan basalts of a mantle plume origin (Xu et al., 2001; Zhong et al., 2011a, 2011b; Song et al., 2013; Liu et al., 2016), ranging from 200 to 400 m thick, are widespread in the region where they unconformably overlie carbonate rocks of the Maokou Formation. After eruption of the basalts, collision between the South China Craton and Indochina Block in Late Triassic produced extensive N- to NE-trending thrust fault-fold system (Zhang et al., 2006; Reid et al., 2007; Han et al., 2012; Zhou et al., 2013c).

3.2. Deposit geology

Major features of the Pb-Zn deposits in this province are summarized in Table 1. The majority of orebodies are vein-type, clearly controlled by faults cutting the Neoproterozoic, Carboniferous and Permian dolostone and limestone sequences (Zhou et al., 2001; J.X. Zhou et al., 2014; M.F. Zhou et al., 2014). Wall rocks commonly exhibit dolomitization, calcification, pyritification, silicification and ferritization (C.Q. Zhang et al., 2005; Chen and Wu, 2012). Ore minerals are mainly sphalerite and galena with minor pyrite, arsenopyrite, chalcopyrite, bornite, cerussite, argentite and bonamite. Gangue minerals include calcite, dolomite and quartz with minor fluorite (Wang et al., 2014; C.Q. Zhang et al., 2015). In addition to Pb and Zn, Ag and Ge are also enriched in some deposits (Ye et al., 2011). The Huize Pb-Zn deposit is the best known and best studied body in the province.

The Huize Pb-Zn deposit in Huize county of Yunnan Province is the largest Pb-Zn deposit in the Chuan-Dian-Qian province. Proven reserves in this deposit include 1.96 million tons of Pb and 2.75 million tons of Zn, at grades of 2.3–9.2% Pb and 2.7–22.5% Zn (Table 1). This deposit also contains an average of about 400 ppm Ge, resulting in about 800 tons of this element.

Sedimentary sequences in the deposit include siliceous dolostone of Neoproterozoic age, overlain by Paleozoic dolostone, limestone, sandstone and greywacke. Permian Emeishan basalts are also present in the mining district. All of the strata were involved in a NE-striking fault-fold system. The ores are mainly hosted in Lower Carboniferous dolostone, which contains 1–5 wt.% SiO_2, probably due to silicification.

Northeast-trending fault-fold system is the dominant structures of the deposit, and the Kuangshanchang and Qilinchang faults controlled the distribution of orebodies. However, sizes, shapes, occurrences of the orebodies mostly depend on secondary structures associated with the major faults (Fig. 3).

More than 30 orebodies are present in this deposit and most occur as NE-trending, steeply dipping veins and lenses along faults in Lower Carboniferous, muddy dolostone (Fig. 4). These orebodies form a mineralized zone, ~800 m long and 1–40 m wide, which extends downdip approximately 1100 m.

Hydrothermal alteration in the deposit is relatively simple, consisting mainly of dolomitization and pyritification with minor calcification, silicification and argillization. Two generations of dolomite are recognized: an early generation of grayish-white, fine- to medium-grained, diagenetic dolomite and a later widespread generation that overprinted the early dolomite to form yellow and beige, euhedral crystals. The dolomitization is closely related to mineralization, and the thicknesses and ore grades of the orebodies increase as dolomitization increases at depth (Chen et al., 2001; Fu, 2004). Pyrite forms cubes and pyritohedron, usually 0.1–0.5 mm in size, with the largest grains being close to the orebodies (Chen et al., 2001; Han et al., 2001; Fu, 2004).

Metallic minerals in the deposit include sphalerite, galena and pyrite, with minor amounts of arsenopyrite, chalcopyrite, bornite, jamesonite, jordanite, argentite, polybasite and aerosite. Gangue minerals are calcite, dolomite and quartz with minor barite and gypsum. Germanium in the deposit is dominantly hosted in sphalerite as an isomorphism component and no Ge minerals have been recognized (Ye et al., 2011).

Three stages of mineralization can be distinguished on the basis of field and petrographic relationships; an early sphalerite-pyrite stage, an intermediate sphalerite-galena stage, and a late pyrite-carbonate stage (Fu, 2004). Mineral assemblages of each stage are summarized in Fig. 5.

Fluid inclusions in sphalerite and calcite from this deposit have been studied extensively (Zhang et al., 2005a, 2005b) and include four types: liquid + gas, gaseous, liquid and multi-phase inclusions with daughter minerals, among which liquid + gas and two-phase inclusions are the most common. Homogenization temperatures are about 130–250 °C, and salinities range from 0.7 to 22.2 wt.% NaCl, but are mostly between 8 and 17 wt.% NaCl. The homogenization temperatures and salinities generally decrease from the early to the late stage (Zhang et al., 2005a, 2005b).

3.3. Origin of the Pb-Zn deposits

A number of different models for the genesis of the Pb-Zn deposits in the Chuan-Dian-Qian province have been proposed. Liu (1996) suggested that the ore-forming materials were from multiple sources, whereas on the basis of Pb and Sr isotopes, Zhou et al. (2001) argued that the ore-forming elements of the Huize Pb-Zn deposit were dominantly from Neoproterozoic strata. Sulfur isotopes of pyrite, sphalerite and galena from the Pb-Zn deposits have been well studied and are similar to those of sulfates in the regional strata, suggesting that the sulfur was derived from sulfates in the strata (X.B. Li et al., 2006). In contrast, W.B. Li et al. (2004) found that the Pb isotopic compositions of sulfides in the ores are similar to those of disseminated pyrite in the carbonate wallrocks, indicating another source of the ore-forming materials. Sulfur isotopes also indicate that the sulfur in the ore-forming fluids was derived from reduced sulfate in the strata.

A histogram of S isotopic compositions of the Pb-Zn deposits in this province shows that different deposits have similar S isotopic compositions with $\delta^{34}S$ values mostly from 8‰ to 20‰ (Fig. 6), similar to the values of marine sulfates of the wallrocks, pointing to this material as the source of sulfur in the fluids. Wen et al. (2016) and Zhu et al. (2013) analyzed Cd and $\delta^{114}Cd$ of different deposits in the region and found that the Pb-Zn deposits hosted in different strata have ore-forming elements derived from their country rocks. Considering the high salinities (as high as 22.2 wt. % NaCl) of the fluids, most researchers agree that the fluids were probably similar to brine waters of MVT Pb-Zn deposits, which were formed from brine fluids rich in ore-forming elements leached from their wallrocks (Zhou et al., 2001, 2013a, 2013b, 2013c, 2015, 2016; J.X. Zhou et al., 2014; M.F. Zhou et al., 2014; Ye et al., 2014; Wen et al., 2016).

4. The Youjiang Au-As-Sb-Hg metallogenic province

4.1. Regional geology

The Youjiang Basin at the southwestern margin of the Yangtze Block is bounded by the Mile-Shizong Fault to the northwest, the Shuicheng-Ziyun-Bama Fault to the northeast, and the Red River Fault to the southwest (Figs. 1 and 7; Cai and Zhang, 2009; Yang et al., 2012; Faure et al., 2014). The oldest unit in this basin is a Cambrian carbonate that crops out within the core of a superposed

Table 1
Major deposits and geological features of the Chuan-Dian-Qian Pb-Zn metallogenic province.

Deposits	County, province	Longitude Latitude	Reserves	Grade	Ore minerals	Gangue minerals	Alterations	Host rocks	Hosting strata	References
Huize	Huize, Yunnan	103°41′55″ 26°38′18″	1.96 Mt Pb 2.75 Mt Zn 800 t Ge	2.3–9.2% Pb 2.7–22.5% Zn	Galena, sphalerite, pyrite, arsenopyrite, chalcopyrite, bornite	Calcite, dolomite, quartz	Dolomitization calcification, silicification, argillization	Dolostone	Early Carboniferous	Chen et al. (2001), Zhou et al. (2001) and Han et al. (2001)
Tianbaoshan	Huili, Yunnan	102°12′07″ 26°57′16″	2.6 Mt (Ores) Pb + Zn	10.1% Zn 1.5% Pb 93.6 g/t Ag	Sphalerite, galena, pyrite, chalcopyrite, cerussite, argentite	Calcite, dolomite	Dolomitization calcification, silicification, sericitization	Dolostone	Neoproterozoic	Wang (1992), Zaw et al. (2007) and Wang et al. (2014)
Daliangzi	Huidong, Sichuan	102°52′05″ 26°37′50″	4.5 Mt (Ores) Pb + Zn	10.4% Zn 0.9% Pb 43.0 g/t Ag	Sphalerite, galena, pyrite	Dolomite, calcite	Silicification, dolomitization calcification,	Dolostone	Neoproterozoic	Zheng and Wang (1991), Zaw et al. (2007) and Wang et al. (2014)
Fule Pb-Zn	Luoping, Yunnan	104°23′53″ 25°21′31″	26,000 t Pb 0.28 Mt Zn	0. 7% Pb 5.1% Zn	Sphalerite, galena, pyrite, arsenopyrite, chalcopyrite, tetrahedrite	Dolomite, calcite	Dolomitization calcification	Dolostone, limestone	Early Permian	Si et al. (2006, 2011)
Shanshulin	Liupanshui, Guizhou	105°04′51″ 26°28′10″	2.7 Mt Pb + Zn	0.5–8.9% Pb 1.1–26.6% Zn	Sphalerite, galena, pyrite	Calcite, dolomite	Dolomitization calcification,	Limestone, dolostone	Late Carboniferous	Wang et al. (2014)
Maomaochang	Hezhang, Guizhou	104°29′34″ 26°58′19″			Galena, sphalerite, pyrite, Cerussite, smithsonite, hydrozincite, hemimorphite, limonite	calcite, dolomite		Dolostone	Early Carboniferous	Zheng (1992) and Chen and Wu (2012)
Caoziping	Hezhang, Guizhou	104°40′11″ 27°00′40″			Galena, sphalerite, chalcopyrite, cerussite, smithsonite	Calcite, dolomite		Dolostone, limestone	Early Carboniferous	Zheng (1992) and Chen and Wu (2012)
Yadu	Hezhang, Guizhou	104°42′33″ 26°59′25″			Galena, sphalerite, pyrite, smithsonite, hydrozincite, hemimorphite, limonite, goethite, chalcopyrite	Calcite, dolomite		Limestone	Early Permian	Zheng (1992) and Chen and Wu (2012)
Mangdong	Hezhang, Guizhou	104°47′25″ 26°55′47″			Galena, sphalerite, pyrite, marcasite, chalcopyrite	Calcite, dolomite		Limestone, clastic rocks	Middle Devonian	Zheng (1992) and Chen and Wu (2012)
Qingshan	Liupanshui, Guizhou	104°53′40″ 26°32′28″			Galena, sphalerite, pyrite, marcasite	Calcite, dolomite	Dolomitization, calcification,	Limestone, dolostone	Late Carboniferous, Early Permian	Zheng (1992) and Chen and Wu (2012)
Maoping	Yiliang, Yunnan	103°59′10″ 27°30′49″	77,000 t Pb 0.165 Mt Zn	5.0% Pb 9.1% Zn	Sphalerite, galena, pyrite	Calcite, quartz, barite	Dolomitization calcification, baritiziation, silicification	Dolostone, limestone	Early Devonian, Middle Carboniferous	Han et al. (2007), Yang et al. (2011, 2012) and Shen et al. (2011)
Maozu	Qiaojia, Yunnan	102°51′03″ 27°18′16″	0.11 Mt Pb 0.72 Mt Zn	1.9% Pb 5.7% Zn	Sphalerite, galena	Calcite, dolomite, quartz, fluorite	Silicification, baritiziation, fluoritization	Dolostone	Neoproterozoic	He et al. (2006), Yang et al. (2012) and Wang et al. (2014)

(*continued on next page*)

Table 1 (*continued*)

Deposits	County, province	Longitude Latitude	Reserves	Grade	Ore minerals	Gangue minerals	Alterations	Host rocks	Hosting strata	References
Tianqiao	Hezhang, Guizhou	104°34′07″ 27°03′48″	0.38 Mt Pb + Zn	16.7% Zn 5.5% Pb	Galena, sphalerite, pyrite, chalcopyrite, marcasite, arsenopyrite, boulangerite	Calcite, dolomite	Dolomitization carbonatization silicification	Limestone	Early Carboniferous	Zheng (1992)
Shaojiwan	Hezhang, Guizhou	104°44′18″ 27°06′12″	0.5 Mt Pb + Zn	0.7–10.6% Pb 2.1–30.4% Zn	Sphalerite, galena, pyrite	Calcite, quartz	Dolomitization, calcification, silicification	Dolostone, limestone	Early Permian	Zhang et al. (2011) and Zhou et al. (2013a)
Jinshachang	Yongshan, Yunnan	103°37′56″ 28°13′03″	4.6 Mt Pb + Zn	41% Pb 5.0% Zn	Sphalerite, galena, pyrite	Calcite, dolomite, quartz, barite, fluorite	Silicification dolomitization baritization, carbonatization chloritization	Dolostone	Neoproterozoic, Early Cambrian	C.Q. Zhang et al. (2005), Guo (2007) and Wang et al. (2014)

anticline (Qiu et al., 2016). It has been suggested that the Youjiang Basin lies on a basement of Lower Paleozoic strata and that it evolved in three stages: passive continental margin rift basin (Early Devonian to Early Permian), back arc basin (Late Permian to Early Triassic) and foreland basin (Middle to Late Triassic), corresponding to the opening, subduction and closing of Paleo-Tethys, respectively (Zeng et al., 1995; Gu et al., 2012; Chen et al., 2015). This basin records significant marine sedimentation between the late Paleozoic and the Middle Triassic (Song et al., 2009), leading to formation of a ~7-km-thick sequence of marine sediments (Galfetti et al., 2008; Yang et al., 2012). After deposition ceased, the sequence was folded to form the EW-trending Youjiang fold-and-thrust belt by Late Triassic Indosinian uplift and northward migration of the basin associated with closure of Paleo-Tethys and subsequent collision between Indochina and South China blocks (Fig. 1; Cai and Zhang, 2009; Yang et al., 2012). Permian and Triassic marine strata, composed of limestone, dolostone, siltstone, sandstone and mudstone, crop out in the basin, and are intruded by ca.-260-Ma diabases in the southern part of the basin. These diabases are thought to be a distal manifestation of the Emeishan mantle plume to the west (M.F. Zhou et al., 2006; Fan et al., 2008). Yanshanian (ca. 90 Ma) and Indosinian (ca. 215 Ma) granite and granite-related W-Sn polymetallic deposits have been recognized in the southern and eastern parts of the basin (Liu et al., 2010; Feng et al., 2011; Cheng, 2013; Chen et al., 2014a; J.W. Zhang et al., 2015; Fig. 7). Gravity and magnetic data indicate the existence of concealed granitic intrusions in the Youjiang Basin, typically at depths of 2–5 km, some of which are up to several tens of km^2 in size (Zhou, 1993).

4.2. Deposit geology

Many low-temperature, hydrothermal Au, As, Sb and Hg deposits have been found within the Youjiang basin and its northeastern margin (Figs. 1 and 7, Table 2), among which Carlin-type gold deposits are the most important. There are more than 200 Carlin-type gold deposits (occurrences) in the province (Hu et al., 2007) with a total proven gold reserve of more than 800 tons, being the second largest such gold mineralized area in the world (Su et al., 2016, in review).

Hosting rocks of the Carlin-type gold deposits are highly variable in age and include Cambrian to Triassic sedimentary rocks (Hu et al., 2002; Table 2). Most of the deposits, however, are hosted in Permian and Triassic sedimentary rocks, the most extensive strata in the basin. On the basis of their occurrence, the Carlin-type orebodies can be classified into two types: strata-bound and fault-bound (Xia, 2005; Su et al., 2008; Chen et al., 2015; Tan et al., 2015). The fault-bound type usually occurs along high-angle reverse faults on the flanks of anticlines or domes, with ores being hosted in calcareous siltstones and silty mudstones, such as those in Lannigou, Yata, and Jinya (Fig. 8). The strata-bound type is controlled by anticlines or domes, with ores hosted in permeable limestone below less-permeable cap rocks or with mineralization along unconformities, such as those in Shuiyindong, Taipingdong and Getang (Fig. 9).

Although the ages and lithologies of the host rocks vary, they share many similarities in terms of mineral assemblages, element associations, hydrothermal alteration and ore-forming conditions.

The Shuiyindong deposit is the largest Carlin-type gold deposit in the region. Recent exploration and underground mining has shown that this deposit has a proven gold reserve of 265 t, with an average grade of 11 ppm Au (Su et al., 2016, in review). It lies on the eastern flank of the Huijiabao anticline where gold deposits also occur on its western flank, including the Zimudang (~80 metric tons) and Taipingdong deposits (Fig. 9). The Shuiyindong deposit is hosted in Permian bioclastic limestone that contains disseminated pyrite and arsenopyrite. Most of the gold occurs in arsenic-bearing pyrite and arsenopyrite as sub-micron particles or lattice gold; some native gold is also present as grains ranging from 0.1 to 6 μm in size (Su et al., 2008, 2012). The geology of the deposit has been described in detail by Su et al. (2008) and Tan et al. (2015).

Reverse faults cut through the axis of the Huijiabao anticline, and are intercepted by N-striking normal faults (Fig. 9), which also control the occurrence of Hg and Tl deposits within this area, such as the Lanmuchang Hg-Tl deposit (Su et al., 2009a). The main orebodies are stratiform or stratiform-like and occur in the core of the anticline, 100–900 m below the surface (Fig. 9).

Hydrothermal alteration in the Shuiyindong gold deposit includes decarbonation, silicification, sulfidation and dolomitization. Ore minerals include arsenic-bearing pyrite, arsenopyrite, realgar, orpiment and stibnite. Gangue minerals are quartz, dolomite, calcite and clay minerals. Three stages of mineralization can be recognized on the basis of field and petrographic relationships (Su et al., 2009a): an early quartz-pyrite stage, an intermediate quartz-arsenian pyrite-arsenopyrite stage and a late quartz-calcite-realgar-orpiment-stibnite stage. Mineral assemblages of each stage are summarized in Fig. 10.

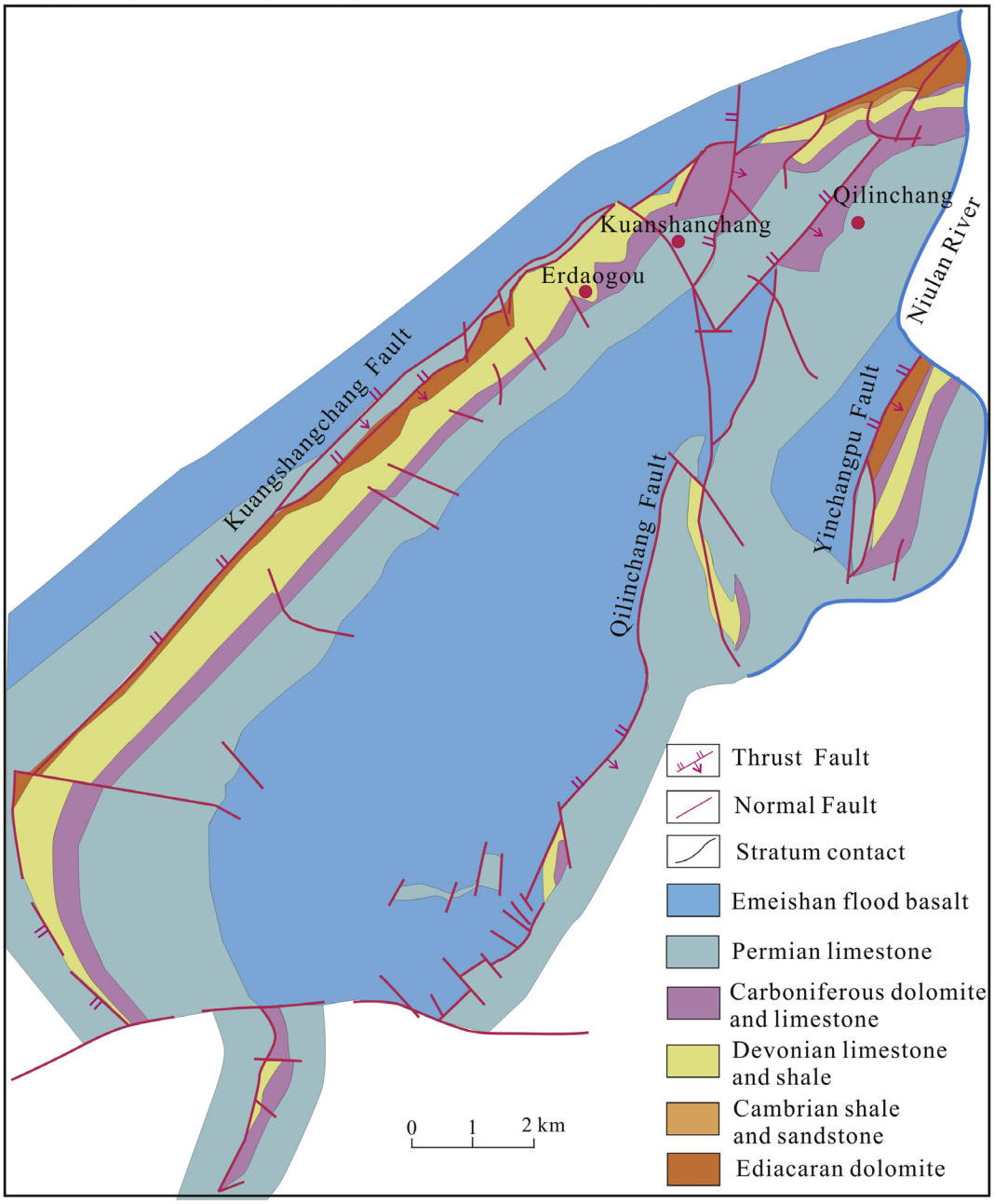

Fig. 3. A geological map of the Huize Pb-Zn deposit (modified from Chen et al., 2001).

Fluid inclusion studies indicate that the ore fluids had low temperatures (126–240 °C) and low salinities (0.2–6.9 wt.% NaCl). Both temperature and salinity decreased from the early to the late stage, but CO_2 increased (Xia, 2005; Su et al., 2009a; Gu et al., 2012).

4.3. Origin of the deposits

Carbon and O isotopic data of calcites from five Carlin-type gold deposits in the Youjiang basin form two trends (Fig. 11). A flat trend between the marine carbonates and granites suggests mixing of CO_2 derived from these two sources (Tan et al., 2015), whereas the sloping trend probably reflects mixing between CO_2 dissolved from the carbonate rocks and CO_2 produced by oxidation of organic matter in the carbonates (Y.W. Peng et al., 2014).

Zhang et al. (2010), Z.P. Wang et al. (2013) and Tan et al. (2015) studied hydrothermal calcites from four Carlin-type gold deposits in the basin, and found that most post-ore calcite grains have positive $\delta^{13}C$ values, whereas calcites of the ore-forming stage have negative values ranging from −3‰ to −9‰, consistent with the values of mantle carbon (−3‰ to −8‰; Rollinson, 1993), suggesting a mantle derivation. However, other possibilities cannot be excluded; e.g., such values could reflect mixing of marine carbonate ($\delta^{13}C \approx 0‰$) and organic carbon ($\delta^{13}C < -20‰$) (Hu et al., 2002).

Hydrogen and O isotopes of quartz and clay minerals from six Carlin-type gold deposits in the Youjiang Basin are plotted in Fig. 12. Although the H and O isotopic values are relatively dispersed, almost all of them plot below the field of metamorphic water, and many lie in the field of formation fluids, indicating that the ore-forming fluids might have been mainly basinal in origin with minor input of metamorphic or magmatic fluids (Y.W. Peng et al., 2014). However, Hofstra et al. (2005) found that the H and

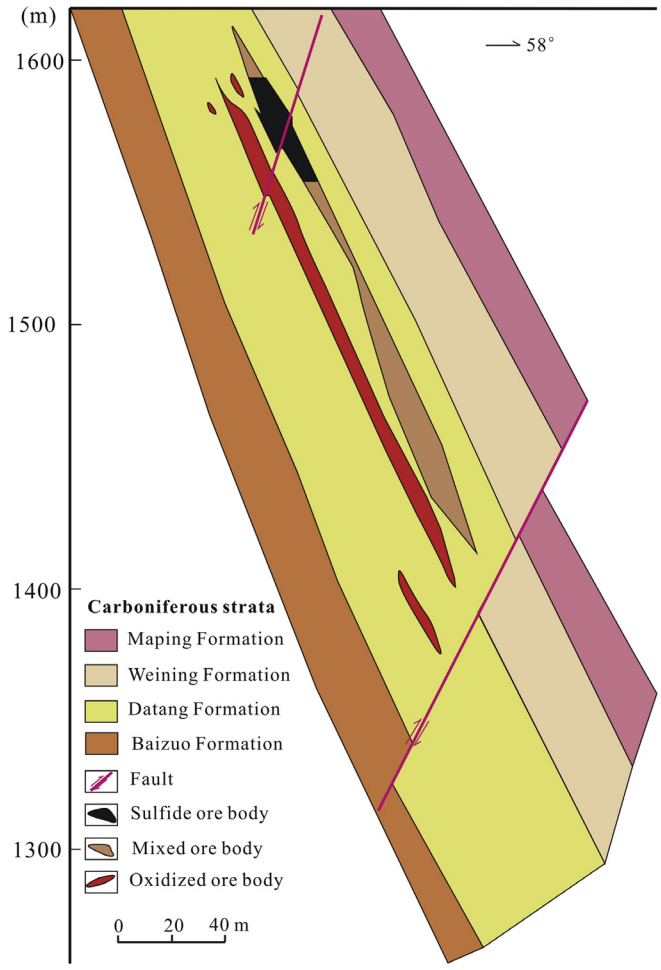

Fig. 4. A cross-section of the main orebodies in the Huize Pb-Zn deposit (Inner geological report).

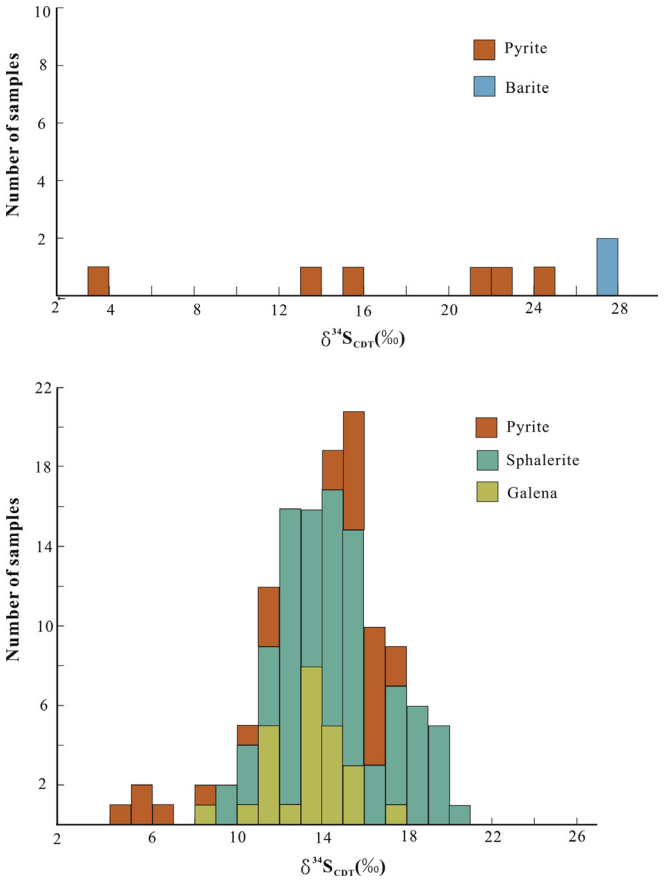

Fig. 6. A histogram of sulfur isotopic compositions in the Pb-Zn deposits of the Chuan-Dian-Qian province (after X.B. Li et al., 2006; Zhou et al., 2013a, 2013b, 2013c).

	Main mineralization			Hypergene oxidized period
	Fe-sphalerite-pyrite stage	Sphalerite-galena stage	Pyrite-carbonate rock stage	
Pyrite				
Sphalerite				
Galena				
Chalcopyrite				
Pyrrhotite				
Arsenopyrite				
Argentite				
Acanthite				
Areosite				
Calcite				
Dolomitee				
Limonite				
Cerusite				
Smithsonite				
Chlorite				
Sericite				

Fig. 5. A paragenetic sequence of minerals in the Huize Pb-Zn deposit (modified from Fu, 2004).

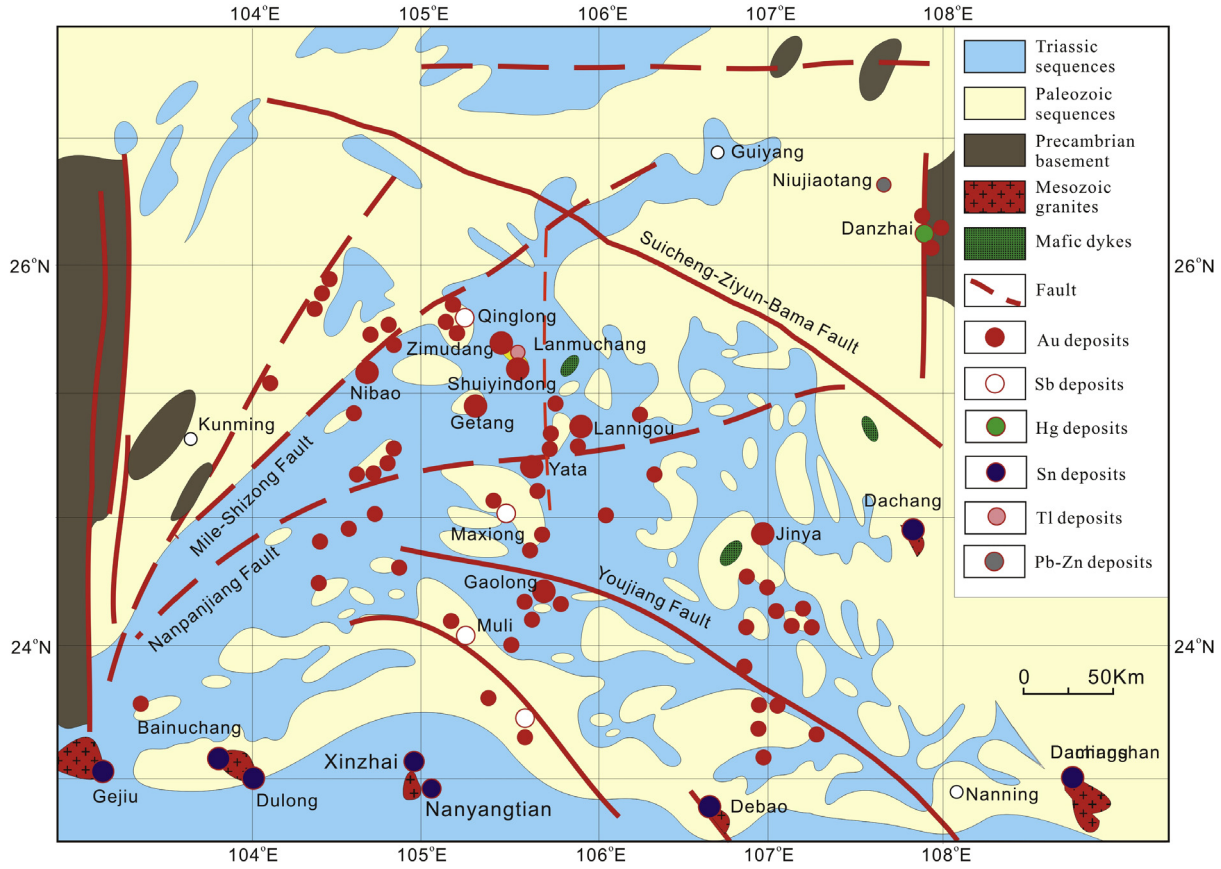

Fig. 7. A map showing the distribution of low-temperature Au-As-Sb-Hg and granite-related, Sn polymetallic deposits in the Youjiang province and adjacent areas (modified from Hu and Zhou, 2012).

O isotopes of clay minerals from several deposits are mostly within the field of metamorphic water or close to its lower boundary, suggesting a metamorphic origin. Furthermore, H and O isotopes of quartz from the Shuiyindong gold deposit mostly plot within the field of magmatic water or close to its lower-left boundary, possibly indicating a magmatic origin although the ore-forming fluid might have been mixed with meteoric fluids during subsequent evolution (Tan et al., 2015).

In earlier studies, pyrite in the Carlin-type gold deposits of the Youjiang basin was considered to be a product of the ore stage. It was concluded that the H_2S was derived from diagenetic dissolution of pyrite because of the similarity in $\delta^{34}S$ values of pyrite from the ore and the host strata (Hu et al., 2002; X.C. Zhang et al., 2005; Fig. 13). However, pyrites in the ores have zoned textures with a diagenetic core and a hydrothermal rim (Fig. 14), indicating that the pyrite is the product of a two-stage process (Su et al., 2008, 2009a).

In order to better understand the sulfur sources, several workers have carried out detailed isotopic analysis of the Shuiyindong gold deposit. For example, Hou et al. (2016) reported that the $\delta^{34}S$ values in the rims of hydrothermal pyrite obtained by SHRIMP in situ analysis range from −2.6 to 1.5‰. In addition, Chen et al. (2014b) analyzed sulfur isotopes of ore-stage, homogeneous arsenopyrite and obtained $\delta^{34}S$ values of 0.8–5.1‰, very similar to those obtained by Z.P. Wang et al. (2013) and Tan et al. (2015) for late-stage sulfides, such as realgar, orpiment and stibnite (−0.5 to 5.3‰). These relatively consistent $\delta^{34}S$ values, −2.6 to 5.3‰, are very close to those of mantle sulfur (0 ± 3‰; Chaussidon et al., 1989), indicating that the sulfur was probably derived from a magmatic source. Actually, except for the Lannigou gold deposit, the $\delta^{34}S$ values of sulfides from most of the gold deposits in the Youjiang Basin are similar to those of the Shuiyindong deposit, with $\delta^{34}S$ being about 0 ± 5‰ (Fig. 15), indicating a deep magmatic source. However, these results cannot exclude the possibility that the H_2S in the ore fluids could also have been derived from an average sedimentary pyrite source, because the mean value of the diagenetic pyrite is essentially 0 ± 5‰ (Hou et al., 2016).

Thus, the sources of the ore-forming fluids of the Carlin-type gold deposits in this region is still unresolved. A magmatic source was commonly excluded in earlier studies because there were no outcrops of igneous rocks, whereas recent studies suggest that magma was probably an important source of the ore-forming fluids in the region. Identification of some concealed granite intrusions in the Youjiang Basin (Zhou, 1993) supports this interpretation.

5. The Xiangzhong Sb-Au metallogenic province

5.1. Regional geology

The Xiangzhong Sb-Au metallogenic province is located at the eastern margin of the Yangtze Block (Fig. 1). The deposits in this province mostly occur on the margin and interior of the Xiangzhong Basin. Between the late Neoproterozoic and early Paleozoic, this area underwent continuous sedimentation for about 400 Ma (Wang and Li, 2003). The early Paleozoic Caledonian orogeny produced ductile shearing, intense folding, granitic magmatism (e.g., Ren, 1991; Faure et al., 2009; Charvet et al., 2010), and the formation of beaded uplifts such as the Baimashan-Longshan, Weishan-Nanyue and Simingshan-Guandimiao uplifts (Liu, 2005; Bai et al.,

Table 2
Major deposits and geological features in the Youjiang Au-As-Sb-Hg metallogenic province.

Deposits	County, province	Longitude Latitude	Reserves	Grade	Ore minerals	Gangue minerals	Alterations	Host rocks	Hosting strata	References
Lannigou	Zhenfeng, Guizhou	105°52′36″ 25°08′40″	167 t Au	4–5 g/t Au	Pyrite, arsenopyrite, stibnite, cinnabar, realgar, orpiment	Quartz, calcite, dolomite, muscovite, clay	Silicification, carbonatization argillization	Fine-grained clastic rocks, limestone, dolomite	Middle Triassic	Chen (2007) and Chen et al. (2009, 2015)
Shuiyindong	Zhenfeng, Guizhou	105°32′40″ 25°31′57″	265 t Au	11.0 g/t Au	Pyrite, arsenopyrite, realgar, orpiment, stibnite, cinnabar, native gold	Quartz, dolomite, calcite, fluorite, sericite, kaolinite, hydromica, asphalt	Decarbonization, silicification, dolomitization	Clastic rocks, limestone	Late Permian	Su et al. (2009a, 2009b)
Taipingdong	Xingren, Guizhou	105°28′45″ 25°33′46″	>29 t Au	4.7 g/t Au	Pyrite, arsenopyrite, realgar, orpiment, stibnite, native gold	Quartz, dolomite, calcite, kaolinite, chlorite, sericite	Silicification, dolomitization, calcification	Limestone, clastic rocks	Late Permian	Qin and Liu (2006) and Liu et al. (2012)
Zimudang	Xingren, Guizhou	105°28′09″ 25°34′15″	80 t Au	6.0 g/t Au	Pyrite, arsenopyrite, realgar, limonite, native gold	Calcite, dolomite, quartz, hydromica, kaolinite, chalcedony	Silicification, dolomitization, calcification	Limestone, fine-grained clastic rocks	Late Permian, Early Triassic	Liu et al. (2009) and Wang (2013)
Nibao	Pu'an Guizhou	104°55′53″ 25°22′24″	43 t Au	2.6 g/t Au	Pyrite, arsenopyrite, realgar, orpiment, stibnite, cinnabar	Quartz, calcite, fluorite, chlorite, sericite, kaolinite	Silicification, carbonatization	Limestone, clastic rocks	Late Permian	P. Liu et al. (2006)
Getang	Anlong, Guizhou	105°17′47″ 25°15′07″	36 t Au	5.0 g/t Au	Pyrite, arsenopyrite, stibnite, realgar, orpiment, limonite	Fluorite, quartz, calcite, dolomite, barite	Silicification, fluoritization, carbonatization,	Limestone, fine-grained clastic rocks	Late Permian	Dong et al. (2011) and Huang et al. (2012b)
Yata	Ceheng, Guizhou	105°39′11″ 24°54′46″	20.7 t Au	5.0 g/t Au	Pyrite, arsenopyrite, realgar, stibnite, chalcopyrite, native arsenic	Quartz, dolomite, calcite, clay	Silicification, carbonatization, argillization	Fine-grained clastic rocks	Middle Triassic	Xiao (2012)
Gaolong	Tianlin, Guangxi	105°39′22″ 24°12′24″	21.6 t Au	3.7 g/t Au	Pyrite, arsenopyrite, stibnite, limonite, valentinite	Calcite, dolomite, quartz, carbon, clay	Silicification, carbonatization, sericitization, kaolinization	Fine-grained clastic rocks	Middle Triassic	Zhang et al. (2012)
Jinya	Fengshan, Guangxi	106°54′23″ 24°34′00″	27.4 t Au	3.4 g/t Au	Arsenopyrite, pyrite, stibnite, realgar, orpiment	Quartz, dolomite, hydromica, calcite	Decarbonization, silicification, argillization	Fine-grained clastic rocks	Middle Triassic	Liu (2013) and Liu et al. (2014)
Mingshan	Lingyun, Guangxi	106°53′00″ 24°21′54″	37.2 t Au	2.7 g/t Au	Pyrite, arsenopyrite, stibnite, chalcopyrite, sphalerite, galena, realgar, orpiment	Quartz, sericite, calcite, dolomite	Silicification, sericitization, argillization	Fine-grained clastic rocks	Middle Triassic	Liang et al. (2015)
Laozhaiwan	Guangnan, Yunnan	104°53′15″ 23°49′30″	31.4 t Au	Au 1.7 g/t Au	Pyrite, arsenopyrite, stibnite, limonite, valentinite	Quartz, sericite, calcite, kaolinite, hydromica, chalcedony	Silicification, carbonatization, sericitization	Fine-grained clastic rocks, diabase	Early Devonian	Luo and Yang (2010), Wang et al. (2011) and J. Zhang et al. (2014)
Dachang	Qinglong, Guizhou	105°08′00″ 25°40′30″	0.274 Mt Sb	2.6% Sb Sb	Stibnite, pyrite, limonite, valentinite	Quartz, fluorite, calcite, kaolinite, barite, gypsum	Silicification, fluoritization, argillization, carbonatization	Clastic rocks	Middle Permian	Peng et al. (2003b) and Su et al. (2015)
Banpo	Dushan, Guizhou	107°37′25″ 25°49′24″	0.15 Mt Sb	5.0–22.3% Sb	Stibnite, pyrite, cinnabar, realgar	Quartz, calcite, dolomite, barite, clay	Silicification, carbonatization, baritization, sericitization	Fine-grained clastic rocks	Early Devonian	Xiao (2014)

Table 2 (*continued*)

Deposits	County, province	Longitude Latitude	Reserves	Grade	Ore minerals	Gangue minerals	Alterations	Host rocks	Hosting strata	References
Banian	Dushan, Guizhou	107°39′15″ 25°46′00″	64,000 t Sb	5.1–6.7% Sb	Stibnite, pyrite	Calcite, dolomite, quartz	Carbonatization, silicification, carbonization	Fine-grained clastic rocks	Middle Devonian	Shen et al. (2013)
Lanmuchang	Xingren, Guizhou	105°30′42″ 25°31′22″	3140 t Hg 392 t Tl	0.19% Hg 0.01% Tl	Cinnabar, lorandite, pyrite, realgar, orpiment, stibnite, christite	Barite, kaolinite, quartz, calcite	Silicification, kaolinization, baritization	Fine-grained clastic rocks	Late Permian, Early Triassic	Chen and Zhou (2000) and Deng (2009)
Jiaoli-La'e	Sandu, Guizhou	107°37′05″, 26°02′30″	>581 t Hg	0.1–3.7% Hg	Cinnabar, realgar, orpiment, pyrite	Calcite, dolomite, barite	Calcification, dolomitization, silicification, baritiziation	Limestone	Early Ordovician	Wang and Wen (2015)

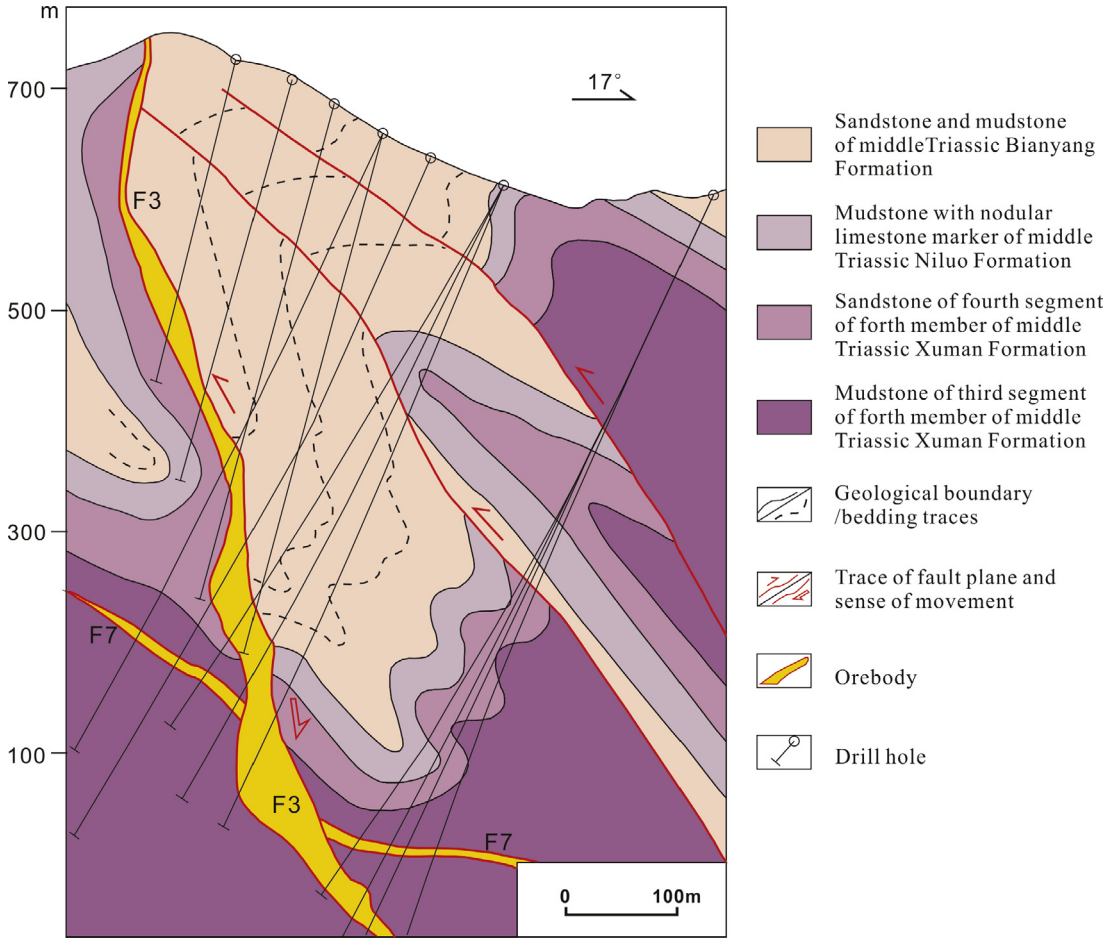

Fig. 8. A cross-section of the Lannigou Carlin-type gold deposit (after M.H. Chen et al., 2011).

2013). Subsequently, the Xiangzhong Basin formed between these uplifts and sedimentation resumed on the Pre-Devonian strata (Fig. 16) composed of metamorphosed clastic rocks, which were unconformable overlain by a marine cover sequence of Late Paleozoic and Early Mesozoic carbonate and clastic rocks (Liu et al., 1985; Shi et al., 1993; Ma et al., 2002). In the Late Triassic, this region was significantly affected by the Indosinian orogeny, leading to the formation of NE-striking structures (called the Xuefengshan belt), the emplacement of granitic plutons and folding of the strata in the basin (e.g., Shu et al., 2009; Chu et al., 2012a, 2012b; Figs. 1 and 16). During a Late Mesozoic tectonic event the earlier structures were reactivated and reworked and the entire Xuefengshan belt was uplifted further (Li et al., 2013). However, igneous rocks of this period are very scarce although geophysical data suggest that some concealed granite intrusions may be present at depth (Li, 1996; Rao et al., 1999).

5.2. Deposit geology

There are more than 170 Sb and Au deposits (occurrences) in this province. The proven Sb reserves are over 2.7 Mt, accounting for more than 50% of the total reserves in the world (J.T. Peng

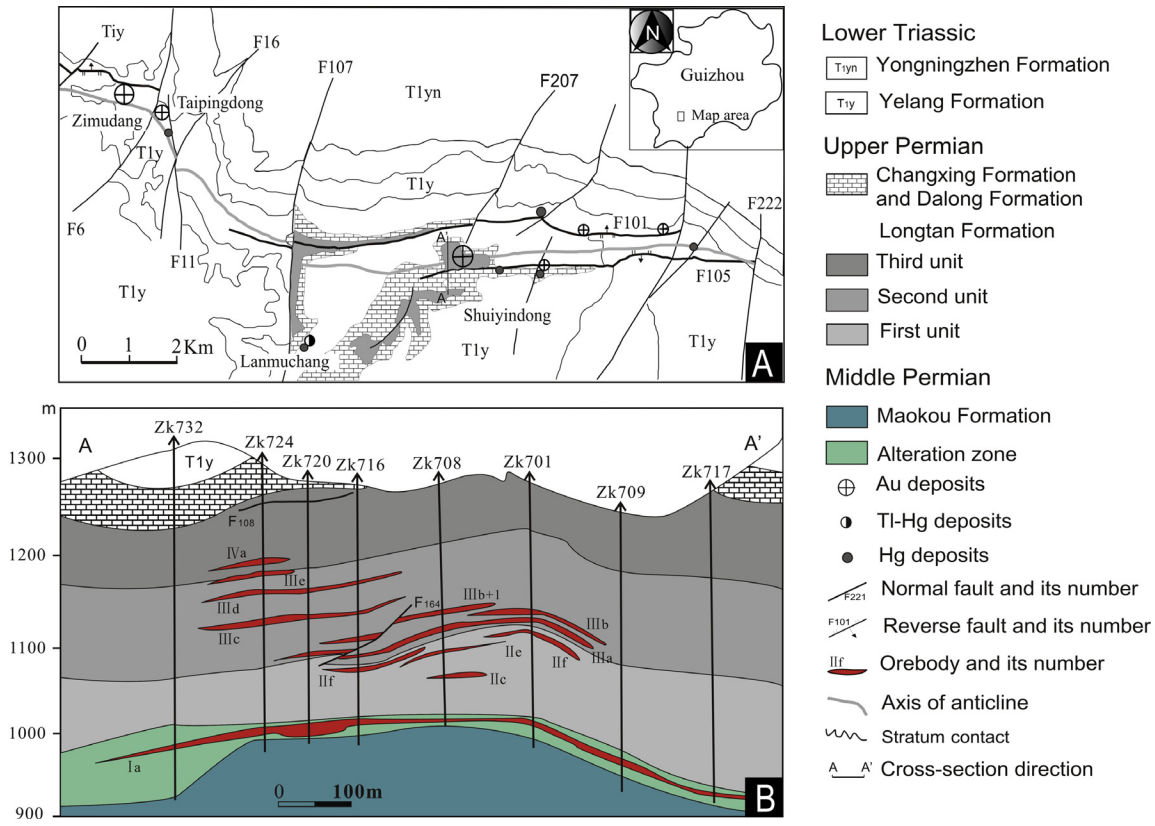

Fig. 9. (A) A map showing the distribution of Au deposits in the Huijiabao anticline (modified from Su et al., 2009b) and (B) cross-section of the Shuiyindong Carlin-type gold deposit (modified from J.Z. Liu et al., 2006).

	Main mineralization		
	Early-stage	Main-stage	Late-stage
Vein quartz			
Arsenic-free pyrite			
Jasperoid quartz			
Arsenic-rich pyrite			
Arsenopyrite			
Marcasite			
Invisible gold			
Native gold			
Dolomite			
Illite and kaolinite			
Stibnite			
Realgar			
Orpiment			
Euhedral quartz			
Vein dolomite			
Vein calcite			

Fig. 10. Paragenetic mineral assemblages in the Shuiyindong Carlin-type gold deposit (modified from Su et al., 2009a).

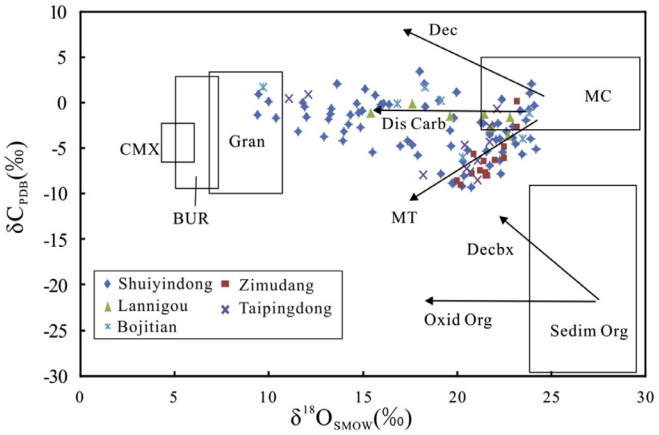

Fig. 11. Carbon and oxygen isotopic compositions of calcites from Carlin-type gold deposits in the Youjiang Au-As-Sb-Hg province. Data are from Zhang et al. (2003, 2010), Z.P. Wang et al. (2013a), Y.W. Peng et al. (2014) and Tan et al. (2015). For reference, the fields for typical marine carbonates (MC), sedimentary organic matter (Sedim Org), igneous carbonatite and mantle xenoliths (CMX), basic and ultrabasic rocks (BUR) and granite (Gran) are outlined. The arrows show typical isotopic trends resulting from carbonate dissolution (Dis Carb), decarbonation (Dec), decarboxylation of organic matter (Decbx), oxidation of organic matter (Oxid Org), and mixing trend (MT).

et al., 2014). On the basis of the host rock ages, the Sb-Au deposits can be classified into two types: Sb deposits occurring in the cover strata of Late Paleozoic carbonate and clastic rocks within the basin, and Sb-Au deposits occurring in the basement of Pre-Devonian, low-grade metamorphic clastic rocks at the margin of the basin (Ma et al., 2002).

The deposits in the cover sequence, such as the Xikuangshan giant Sb deposit, usually occur as stratabound features in Devonian limestone far from any known granite bodies. Their mineral assemblages are relatively simple, with stibnite as the major ore mineral and quartz and calcite as the main gangue minerals. Wallrock alteration is mainly silicification and carbonation (Table 3).

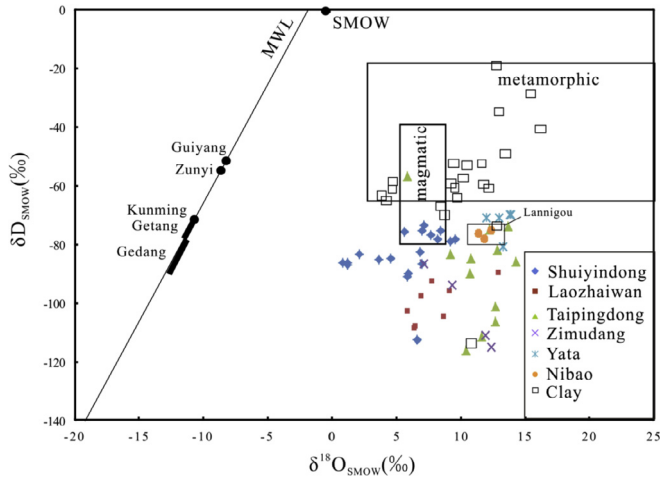

Fig. 12. Hydrogen and oxygen isotopic compositions of water in ore fluids based on analyses of quartz and clay minerals from Carlin-type gold deposits in the Youjiang Au-As-Sb-Hg province (data are from Hu et al., 2002; Hofstra et al., 2005; Wang, 2013; Y.W. Peng et al., 2014; J. Zhang et al., 2014; Tan et al., 2015). MWL represents Meteoric Water Line.

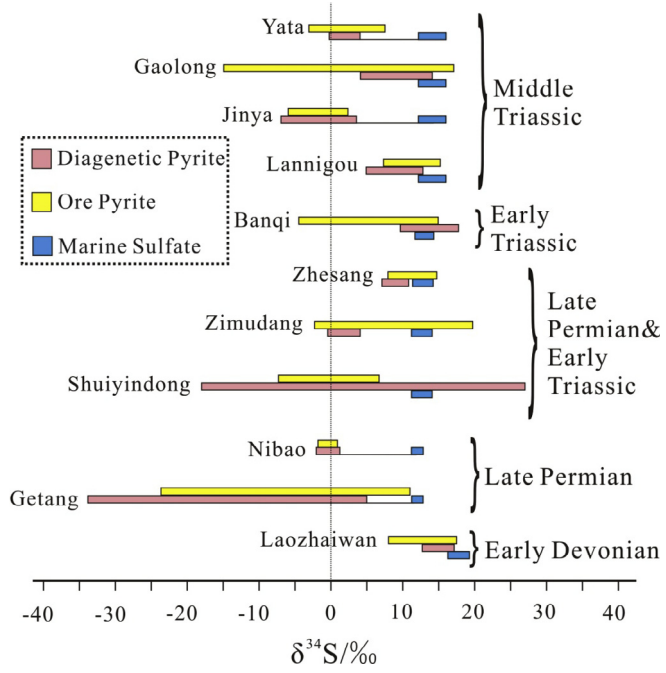

Fig. 13. Conventional sulfur isotopic analyses of diagenetic pyrite and pyrite from various ores. The hosting strata and corresponding sulfur isotopic composition of marine sulfate are also presented (data are from Chen, 2001; Hu et al., 2002; Zhang et al., 2003, 2005d; P. Liu et al., 2006; Nie, 2007; Yao, 2008; Xia et al., 2009; C.H. Wang et al., 2010; Huang et al., 2012a; Z.P. Wang et al., 2013; Y.M. Zhang et al., 2013; Dai et al., 2014; Y.W. Peng et al., 2014; J. Zhang et al., 2014; Tan et al., 2015; Liu, 2015; Hou et al., 2016).

The deposits in basement rocks are usually small, with only the Banxi, Longshan, Gutaishan and Gaojia'ao deposits being of significant sizes. Most orebodies are vein type, and are located either around known granite intrusions, such as the Gutaishan and Qingjingzhai gold deposits, or above concealed granite intrusions, such as the Longshan Sb-Au and Daxin gold deposits. Mineral assemblages in these deposits are relatively complicated with stibnite, native gold, pyrite, arsenopyrite and scheelite as the main ore minerals. Hydrothermal alteration mainly includes silicification, sericitization and chloritization. The features of the Sb-Au deposits in this province are summarized in Table 3. The following are some details of the Xikuangshan Sb deposit, the most important deposit of the province.

The deposit, with a Sb reserve of about 2.5 Mt, is located within the Xiangzhong Basin (Fig. 16), where it is associated with carbonates and minor siltstone and mudstone of Early Carboniferous and Middle-Late Devonian ages (Fig. 16). The orebodies are hosted in the Middle-Late Devonian sedimentary rocks (Hu et al., 1996; Fan et al., 2004; Peng et al., 2003a), where mudstone layers above the carbonates are thought to have acted as a barrier to the rise of ore fluids, resulting in the precipitation and accumulation of Sb in the limestone (Jin et al., 2001; R.Y. Yang et al., 2006; Chen, 2012).

Four secondary anticlines of the Xikuangshan complex anticline controlled the distribution of orebodies in the Feishuiyan, Wuhua, Laokuangshan and Tongjiayuan ore blocks (Fig. 17; Hu et al., 1996; Kuang, 2000). More than 80% of the Sb reserves come from strata-bound orebodies, which were controlled by interlayer fault zones in silicified carbonates (Wen et al., 1993; Xie et al., 1996; Tang et al., 1999; Kuang, 2000; He et al., 2002; Chen, 2012; Fig. 17). Secondary barite and fluorite are also locally present (Kuang, 2000; He et al., 2002).

Mineral assemblages are relatively simple with stibnite as the main ore mineral, which is accompanied by minor pyrite. Gangue minerals are mainly quartz and calcite along with minor barite, fluorite and gypsum (Fan et al., 2004; Hu et al., 1996; Peng et al., 2003a). On the basis of mineral associations, three stages of mineralization are recognized; pre-ore, ore-forming and post-ore, with mineral assemblages of each stage shown in Fig. 18.

Fluid inclusion studies of hydrothermal quartz and calcite indicate that the ore-forming fluids had low temperatures and low salinities. The homogenizing temperatures of the fluid inclusions are commonly between 140 and 250 °C, and the salinities are typically lower than 5 wt.% NaCl (Lu et al., 2000; Jin et al., 2001; Ma et al., 2003; Wu et al., 2007).

5.3. Origin of the deposits

The origin of the deposits in the Xiangzhong Sb-Au province has long been controversial. Both granite-related (Liu et al., 1985; Yang, 1986; Lu, 1999; Murao et al., 1999) and granite-unrelated (Chen et al., 1983; Liang, 1991; Liu, 1992; Wen et al., 1993; Fan et al., 2004; D.S. Yang et al., 2006) models have been proposed.

In a δD-δ^{18}O diagram of fluid inclusions trapped in hydrothermal quartz and calcite (Fig. 19), most samples plot between the fields of magmatic and meteoritic water, suggesting mixing of the two components. However, the Mesozoic deposits in South China most likely formed from meteoric water which had δD and δ^{18}O values of approximately -60 ± 10‰ and -9‰, respectively (Zhang, 1989). The δD-δ^{18}O compositions of the ore-forming fluids could be also interpreted as a result of water-rock interaction between Mesozoic meteoric water and δ^{18}O-enriched sedimentary rocks. Thus, the δD-δ^{18}O compositions cannot provide a definitive explanation for the origin of the ore-forming fluids. However, as discussed below there may be some basic differences between the Sb deposits in the late Paleozoic sedimentary rocks and the Sb-Au deposits in the Pre-Devonian, low-grade metamorphic rocks.

Ma et al. (2002, 2003) reported that relatively 'fresh' sedimentary rocks hosting some of the Sb deposits, such as those of the Xikuangshan deposit, generally have very low Sb contents (average 0.9 ppm), whereas the Sb contents range up to 46 ppm in 'altered' host rocks, indicating an external source of Sb. In contrast, the Sb and Au in deposits hosted in the metamorphic basement rocks, such as Longshan, show a U-shaped pattern going from "fresh" rocks to altered rocks and ores, demonstrating that the metals were derived from the altered country rocks. Furthermore, REE

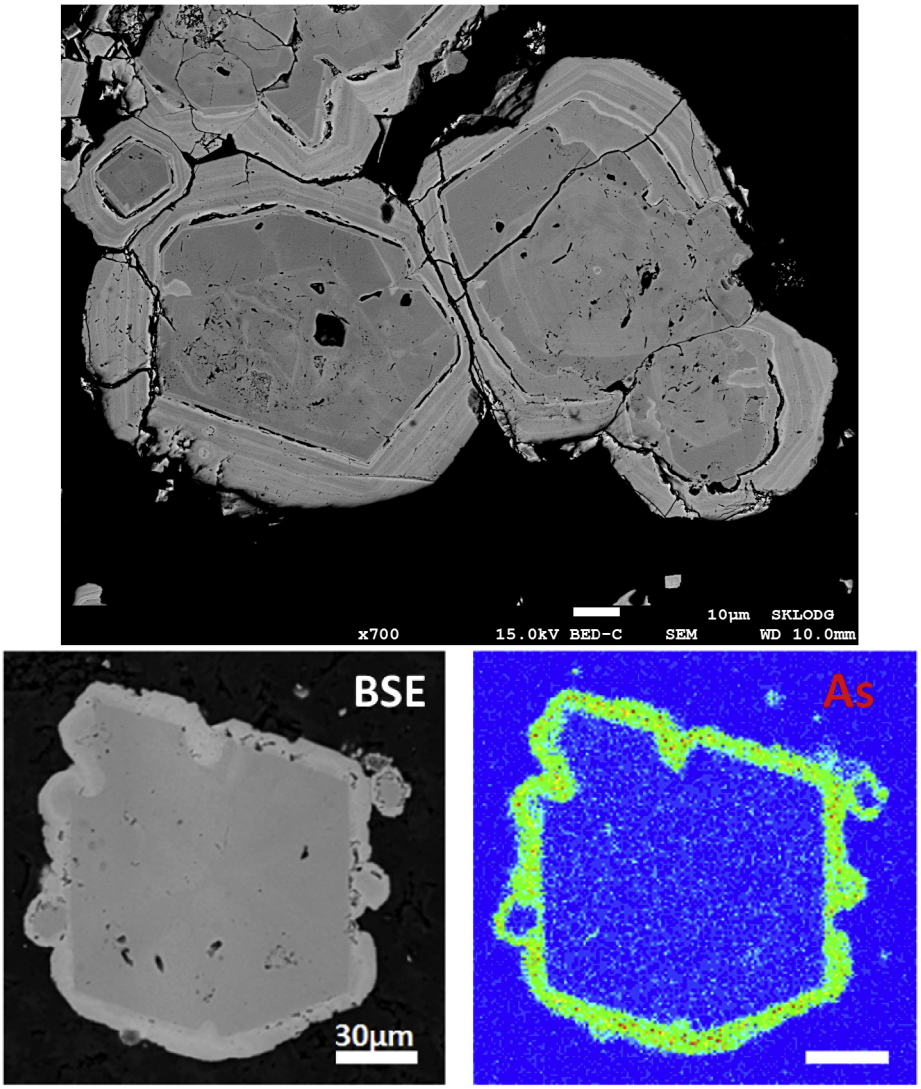

Fig. 14. BSE image and arsenic mapping of Au-bearing pyrite from the Shuiyindong deposit, with As-poor pyrite core overgrown by As-rich rim.

patterns of stibnite from deposits in the cover strata are different from those of their host rocks (Ma et al., 2002). In contrast, the REE patterns of stibnite from Sb deposits in the cover strata and Sb-Au deposits in the basement strata are all similar to those of the basement metamorphic rocks (Ma et al., 2002). These differences suggest that the ore-forming elements of both the Sb and Au-Sb deposits might have been derived from the basement rocks.

The S isotopic compositions of sulfides in the two types of deposits are different from each other. $\delta^{34}S$ values of stibnite from the Sb deposits vary between −2.8 and +16.3‰, mostly +5 to +10‰ (Fig. 20a), whereas the isotopic compositions of sulfides from the Sb-Au deposits are very homogeneous with $\delta^{34}S$ values of about. −2.0 to +2.0‰ (Fig. 20b). There are almost no sulfate minerals in these deposits, implying that the measured $\delta^{34}S$ values of the sulfides reflect those of the total sulfur in the ore-forming fluids (Ohmoto and Rye, 1979). The different $\delta^{34}S$ values of sulfides from the different types of deposits indicate different sources. The sulfur isotopes of the Sb deposits, such as the Xikuangshan, are similar to those of sulfides from the basement strata (Fig. 21), indicating a likely source of sulfur for mineralization. In contrast, the $\delta^{34}S$ values of Sb-Au deposits, such as the Longshan, Gutaishan and Daxin, are about 0‰, suggesting that the sulfur in these deposits was magmatic in origin (Ohmoto, 1986).

The differences in the S isotopes of the two types of deposits are mirrored in the C isotopes of calcites from the deposits. In the Xikuangshan Sb deposit all measured calcite grains, except those of the early stage that have magma-derived $\delta^{13}C$ values of −7 to −6.1‰, have $\delta^{13}C$ values of −0.9 to +2.1‰, similar to those of the host carbonate rocks, indicating derivation from that source (Peng and Hu, 2001a; Peng et al., 2002; Ma et al., 2003). However, the $\delta^{13}C$ values of fluid inclusions trapped in quartz from the Sb-Au deposits vary between −7.5 and −7.8‰, suggesting that those ore-forming fluids might have been magma-derived (Taylor, 1986).

In conclusion, the Sb-Au deposits hosted in the basement rocks may have formed from magmatic fluids, which leached the ore-forming elements from the basement metamorphic rocks. In contrast, the Sb deposits in the cover strata probably were derived dominantly from meteoric fluids rich in sulfur and CO_2 derived from the host rocks, although minor amounts of magmatic fluid might have been involved in the early stage mineralization. However, some of the ore-forming elements of the deposits in the cover sequences were probably also derived from the basement rocks due to interaction between the rocks and circulating meteoric fluids. This interpretation is supported by the observation that the Sb-Au deposits usually occur near known granitic intrusions, whereas

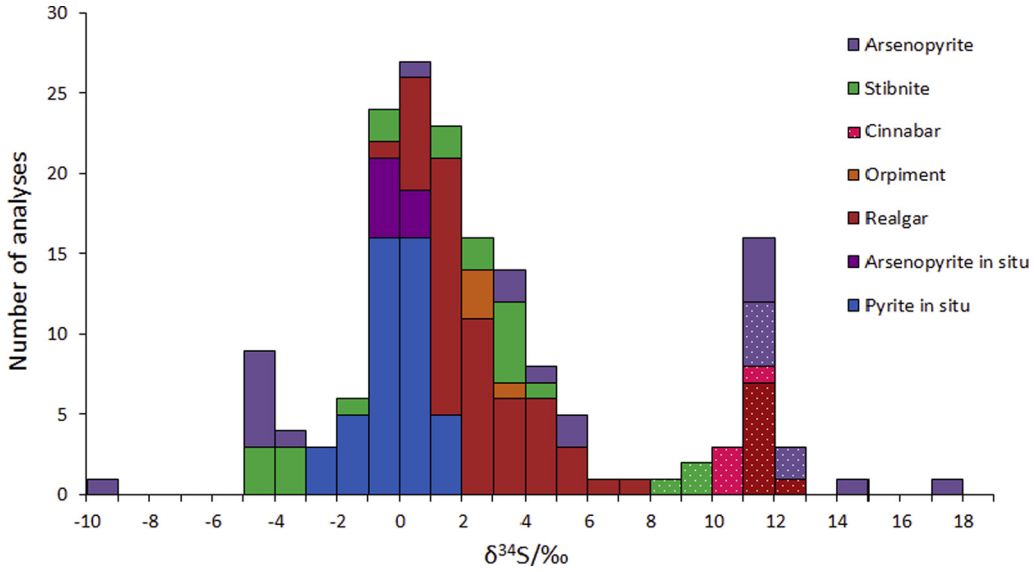

Fig. 15. A summary of reliable sulfur isotopic values for sulfides of Carlin-type gold deposits in the Youjiang Au-As-Sb-Hg province (data from Zhang et al., 2003, 2010; Z.P. Wang et al., 2013; Y.M. Zhang et al., 2013; Y.W. Peng et al., 2014; Chen et al., 2014b; J. Zhang et al., 2014; Liu, 2015; Tan et al., 2015; Hou et al., 2016). White-dotted bars represent data from the Lannigou deposit. The other bars represent data from the Shuiyindong, Taipingdong, Zimudang, Getang, Yata, Jinya, Zhesang and Laozhaiwan deposits.

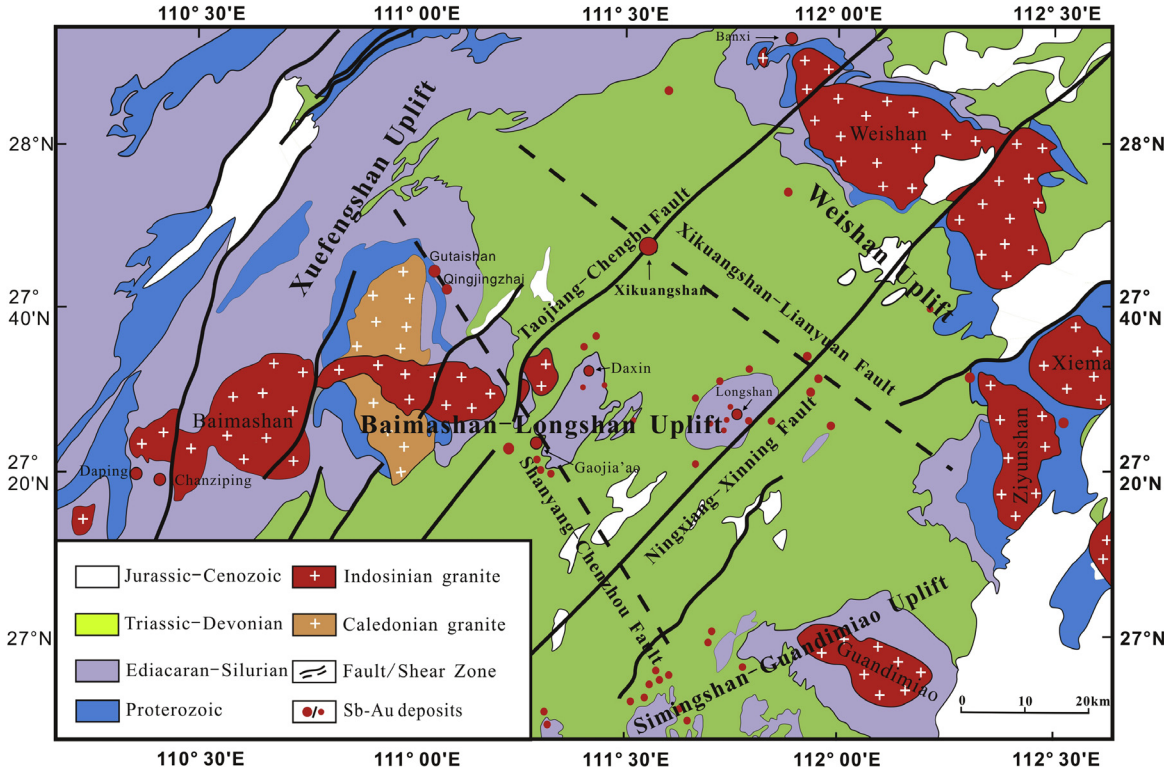

Fig. 16. A map showing the distribution of Sb-Au deposits in the Xiangzhong Sb-Au province (modified from BGMRHN, 1988; Tao et al., 2001; J.H. Li et al., 2004).

no such intrusions have been recognized in the vicinity of the Sb deposits.

6. Genetic links between mineralization and igneous events

A common problem of low-temperature hydrothermal deposits hosted in sedimentary rocks is the lack of suitable minerals for traditional radiometric dating, making it difficult to determine the precise ages of the deposits (Arehart et al., 2003; Li et al., 2003). Because the ages of mineralization were previously unknown, it was formerly not possible to link large-scale, low-temperature mineralization and geological events in South China. However, some progress has been achieved in recent years due to improvements in dating techniques and the discovery of some additional datable minerals (Table 4).

Table 3
Major deposits and geological features of the Xiangzhong Sb-Au metallogenic province.

Clusters	Deposits	County, province	Longitude Latitude	Reserves	Grade	Ore minerals	Gangue minerals	Alterations	Host rocks	Host rock ages	References
Xiangzhong Sb-Au	Xikuangshan	Lengshuijiang, Hunan	111°27′30″ 27°44′30″	2.49 Mt Sb	3.5–5.7% Sb	Stibnite, pyrite, valentinite	Quartz, calcite, gypsum, fluorite, barite	Silicification, carbonatization, baritiziation, fluoritization,	Limestone, fine-grained clastic rocks	Late-Middle Devonian	Hu et al. (1996) and Peng et al. (2003a)
	Banxi	Taojiang, Hunan	111°54′22″ 28°21′03″	0.12 Mt Sb	15.3–25.9% Sb	Stibnite, pyrite, arsenopyrite, chalcopyrite, sphalerite, native gold	Quartz, chlorite, sericite, dolomite	Silicification, chloritization, sericitization, carbonatization	Low-grade metamorphic clastic rocks	Neoproterozoic	Hu (1991) and Luo (1995)
	Longshan	Shaoyang, Hunan	111°39′30″ 27°27′00″	0.10 Mt Sb 10 t Au	4.9–22.8% Sb 3.0–4.8 g/t Au	Stibnite, native gold, arsenopyrite, pyrite, valentinite	Quartz, sericite, feldspar, dolomite, calcite	Silicification, sericitization, carbonatization	Low-grade metamorphic clastic rocks	Neoproterozoic	Liang (1991), Liu et al. (2008) and Pang et al. (2011)
	Daxin	Xinshao, Hunan	111°25′26″ 27°32′33″	>30 t Au	1.0–6.1 g/t Au	Pyrite, arsenopyrite, native gold, chalcopyrite, sphalerite, hematite, siderite	Quartz, sericite, calcite, chlorite, feldspar	Silicification, sericitization, chloritization	Low-grade metamorphic clastic rocks	Neoproterozoic	Gong et al. (2007) and Li (2007)
	Gaojia'ao	Xinshao, Hunan	111°18′01″ 27°25′09″	>10 t Au	1.8–5.1 g/t Au	Native gold, pyrite, marcasite, sphalerite, arsenopyrite, siderite	Quartz, sericite, clay	Silicification, sericitization, baritiziation	Fine-grained clastic rocks	Middle Devonian	Kang (2001) and Li et al. (2002)
	Gutaishan	Xinhua, Hunan	111°04′55″ 27°48′05″	>30 t Au	13.0 g/t Au	Native gold, pyrite, chalcopyrite, arsenopyrite, scheelite	Quartz, sericite, calcite, barite, ferrodolomite	Sericitization, chloritization, carbonatization, silicification	Low-grade metamorphic clastic rocks	Neoproterozoic	Yu (1998) and Dai (2000a)
	Qingjingzhai	Xinhua, Hunan	111°04′05″ 27°42′53″	55 t Au	3.0–14.7 g/t Au	Pyrite, arsenopyrite, native gold, chalcopyrite, limonite,	Quartz, feldspar, sericite, chlorite, calcite, clay	Silicification sericitization, chloritization	Low-grade metamorphic clastic rocks	Neoproterozoic	Dai (2000a, 2000b)
	Chanziping	Qianyang, Hunan	110°22′06″ 27°19′40	29 t Au	1.0–4.9 g/t Au	Pyrite, arsenopyrite, native gold, chalcopyrite, galena	quartz, sericite, chlorite, tourmaline	silicification sericitization, greisenization	Low-grade metamorphic clastic rocks	Neoproterozoic	Li et al. (2008) and Cao et al. (2014, 2015)
	Daping	Hongjiang, Hunan	110°17′31″ 27°21′01″	Au 30 t	Au3.3–22.3 g/t	Native gold, pyrite, arsenopyrite, sphalerite	Quartz, sericite	Silicification sericitization	Low-grade metamorphic clastic rocks	Neoproterozoic	Zhao (2001) and Li et al. (2008)

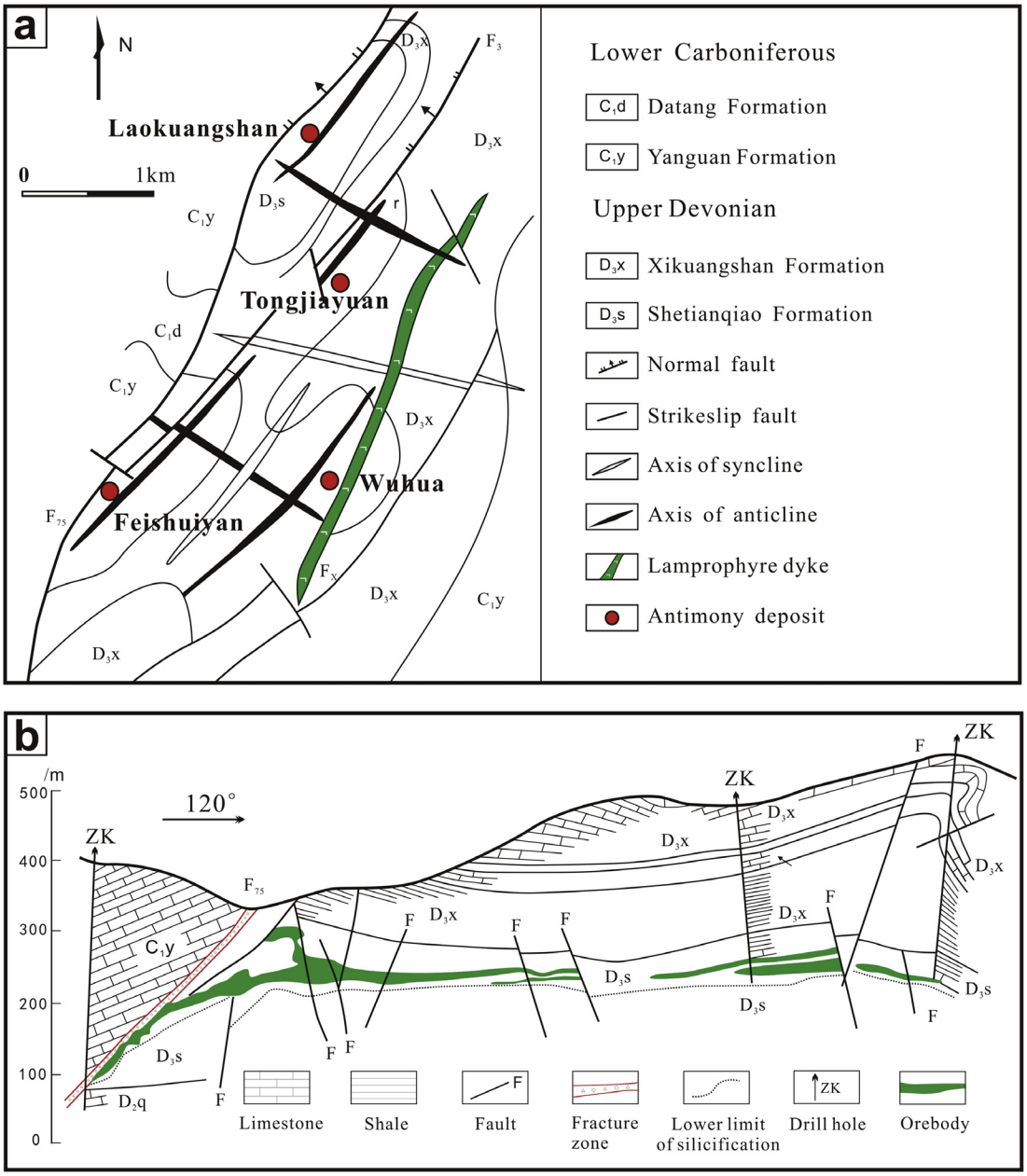

Fig. 17. (a) A geological map of the Xikuangshan Sb deposit (modified from Peng and Hu, 2001a) and (b) a typical cross-section of the Xikuangshan Sb deposit (modified from Jin, 2002; Tao et al., 2002).

	Pre-mineralization	Main mineralization			Post-mineralization
		Early stage	Middle-stage	Late-stage	
Quartz					
Calcite					
Stibnite					
Pyrite					
Barite					
Fluorite					
Gypsum					

Fig. 18. A paragenetic sequence of minerals from the Xikuangshan Sb deposit (after Lin, 2014).

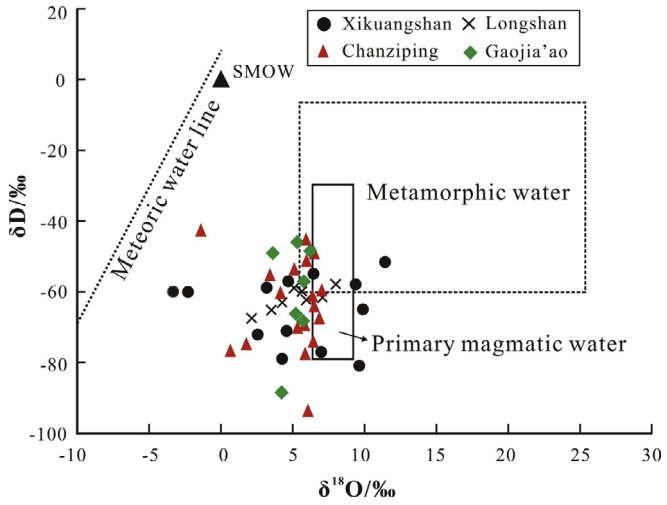

Fig. 19. H-O isotopic compositions of the Sb-Au deposits in the Xiangzhong province. .

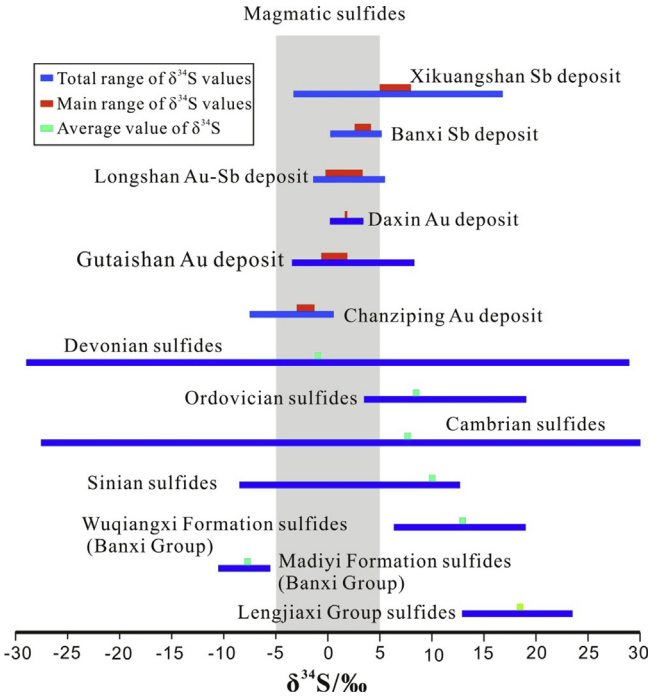

Fig. 21. Comparison of sulfur isotope compositions between deposits in the Xiangzhong Sb-Au province and those elsewhere (data from Liu et al., 1985; Ohmoto, 1986; Jiang et al., 1990; Liu, 1992; Ma et al., 2003; D.S. Yang et al., 2006).

6.1. Chuan-Dian-Qian Pb-Zn province

Using Sm-Nd isotopes of calcite associated with ore minerals from the Qilinchang and Kuangshanchang orebodies in the Huize Pb-Zn deposit, W.B. Li et al. (2004) obtained isochron ages of 226 ± 15 Ma and 225 ± 38 Ma, respectively. C.Q. Zhang et al. (2005) obtained a K-Ar age of 176.5 ± 2.5 Ma on hydrothermal clay minerals from the Huize Pb-Zn deposit, whereas Zhou et al. (2013b, 2013c) reported Rb-Sr isochron ages of 191.9 ± 6.9 Ma and 196 ± 13 Ma for sphalerite from the Tianqiao and Maozu Pb-Zn deposits, respectively. All the ages summarized here are plotted in Fig. 22, which shows that the ore deposits in the province probably formed dominantly between 200 and 230 Ma, corresponding to the Late Indosinian.

6.2. Youjiang Au-as-Sb-Hg province

Some important progress has also been made in dating the Carlin-type gold deposits. Chen et al. (2009) dated sericite in quartz veins from the Lannigou deposit, and obtained a $^{40}Ar/^{39}Ar$ plateau age of 194.6 ± 2 Ma. Using Re-Os isotopes of arsenopyrite from the Lannigou, Jinya and Shuiyindong deposits, Chen et al. (2015) reported ages of 204 ± 19 Ma, 206 ± 22 Ma and

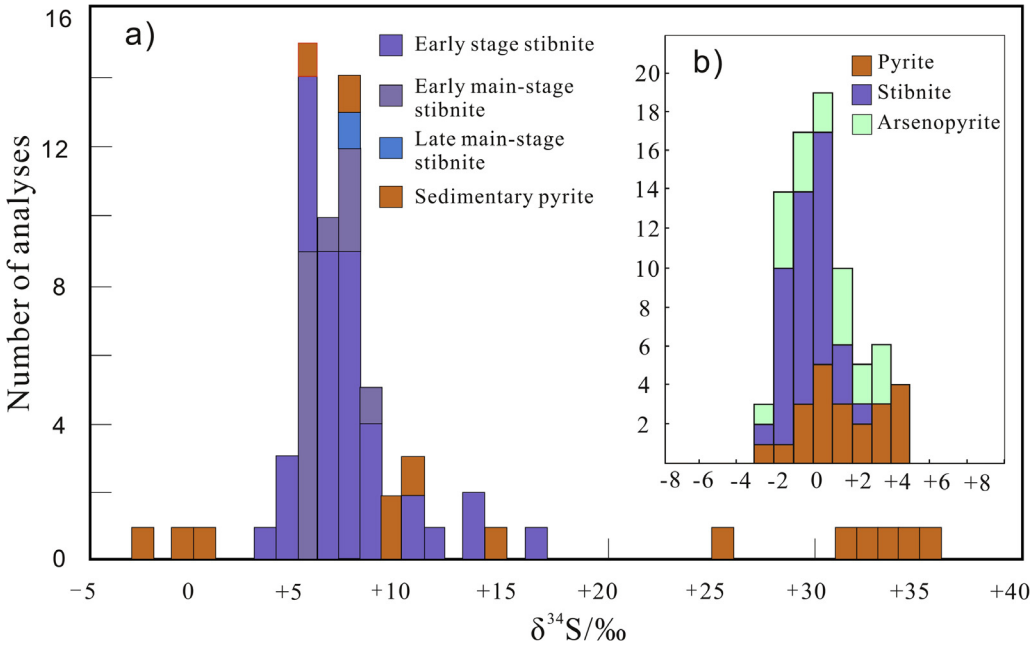

Fig. 20. (a) Sulfur isotopes of sulfides from the Xikuangshan Sb deposit (after D.S. Yang et al., 2006) and (b) sulfur isotopic composition of hydrothermal sulfides from the Longshan Sb-Au deposit (after Ma et al., 2003).

Table 4
Age summary of major deposits in the South China LTMD.

Provinces	Deposits	Ages (Ma)	Methods	References
Chuan-Dian-Qian Pb-Zn	Huize	226 ± 15, 225 ± 38	Calcite Sm-Nd	W.B. Li et al. (2004)
		176.5 ± 2.5	Clay mineral K-Ar	C.Q. Zhang et al. (2005)
		223.5 ± 3.9, 226 ± 6.4	Sphalerite Rb-Sr	Yin et al. (2009)
		196.3 ± 1.8	Sphalerite Rb-Sr	C.Q. Zhang et al. (2014)
	Tianqiao	191.9 ± 6.9	Sphalerite Rb-Sr	Zhou et al. (2013a)
	Maozu	196 ± 13	Calcite Sm-Nd	Zhou et al. (2013b)
	Chipu	292.0 ± 9.7, 165.7 ± 9.9	Bitumen Re-Os	Wu (2013)
	Daliangzi	204.4 ± 1.2	Calcite Sm-Nd	Wu (2013)
	Jinshachang	201.1 ± 6.2	Fluorite Sm-Nd	J.W. Zhang et al. (2015) and Wu (2013)
		206.8 ± 3.7	Sphalerite Rb-Sr	Zhou et al. (2015)
	Lehong	200.9 ± 8.3	Sphalerite Rb-Sr	Y.X. Zhang et al. (2014)
	Paoma	200 ± 1	Sphalerite Rb-Sr	Lin et al. (2010)
	Tianbaoshan	>166	Zircon U-Pb age of diabase	R. Wang et al. (2012)
Youjiang Au-As-Sb-Hg	Shuiyindong	235 ± 33	Arsenopyrite Re-Os	Chen et al. (2015)
		134 ± 3, 136 ± 3	Calcite Sm-Nd	Su et al. (2009b)
	Lannigou	204 ± 19	Arsenopyrite Re-Os	Chen et al. (2015)
		194.6 ± 2	Sericite $^{40}Ar/^{39}Ar$	Chen et al. (2009)
	Jinya	206 ± 22	Arsenopyrite Re-Os	Chen et al. (2015)
	Zhesang	213.6 ± 4.6	Rutile U-Pb	Pi et al. (2016, in review)
		215.3 ± 1.9	Sericite $^{40}Ar/^{39}Ar$	Pi et al. (2016, in review)
	Laozhaiwan	216.9 ± 3.4, 223.9 ± 6.9, 207.9 ± 5.9	Monazite U-Pb	Pi et al. (2016, in preparation)
	Zimudang	148.4 ± 4.8	Calcite Sm-Nd	Wang (2013)
	Qinglong	148 ± 8, 142 ± 16	Fluorite Sm-Nd	Peng et al. (2003b)
	Banian	126.4 ± 2.7, 128.2 ± 3.2	Calcite Sm-Nd	Wang (2012)
	Banpo	130.5 ± 3	Calcite Sm-Nd	Xiao (2014)
	Jiaoli-La'e	129 ± 20	Calcite Sm-Nd	Wang and Wen (2015)
Xiangzhong Sb-Au	Chanziping	205.6 ± 9.4	Quartz fluid inclusion Rb-Sr	Li et al. (2008)
	Daping	204.8 ± 6.3	Quartz fluid inclusion Rb-Sr	Li et al. (2008)
	Fuzhuxi	209	Host granite porphyry K-Ar	Yao and Zhu (1993)
	Liaojiaping	200	Host granite K-Ar	Xiao et al. (1992)
	Banxi	194–202	Host granite porphyry K-Ar	Peng and Hu (2001b)
	Xikuangshan	156.3 ± 12	Calcite and stibnite Sm-Nd	Hu et al. (1996)
		155.5 ± 1.1	Calcite Sm-Nd	Peng et al. (2003a)

235 ± 33 Ma respectively. Pi et al. (2016, in review) dated hydrothermal rutile and sericite from the Zhesang gold deposit, and obtained an in situ U-Pb isochron age of 213.6 ± 4.6 Ma for the rutile and a $^{40}Ar/^{39}Ar$ plateau age of 215.3 ± 1.9 Ma for the sericite. Pi et al. (2016, in preparation) also analyzed hydrothermal monazite in three samples from the Laozhaiwan gold deposit, and obtained in situ U-Pb isochron ages of 216.9 ± 3.4 Ma, 223.9 ± 6.9 Ma and 207.9 ± 5.9 Ma, consistent with the $^{40}Ar/^{39}Ar$ age of sericite, the Re-Os age of arsenopyrite and the U-Pb ages of rutile.

Calcite from the Shuiyindong gold deposit has Sm-Nd isochron ages of 134 ± 3 Ma and 136 ± 3 Ma (Su et al., 2009b). Y.J. Wang et al. (2013) reported a Sm-Nd isochron age of 148.4 ± 4.8 Ma for calcite from the Zimudang gold deposit, whereas Peng et al. (2003b) reported a Sm-Nd age of 148 ± 8 Ma for fluorite from the Qinglong Sb deposit. Wang (2012) obtained two Sm-Nd isochron

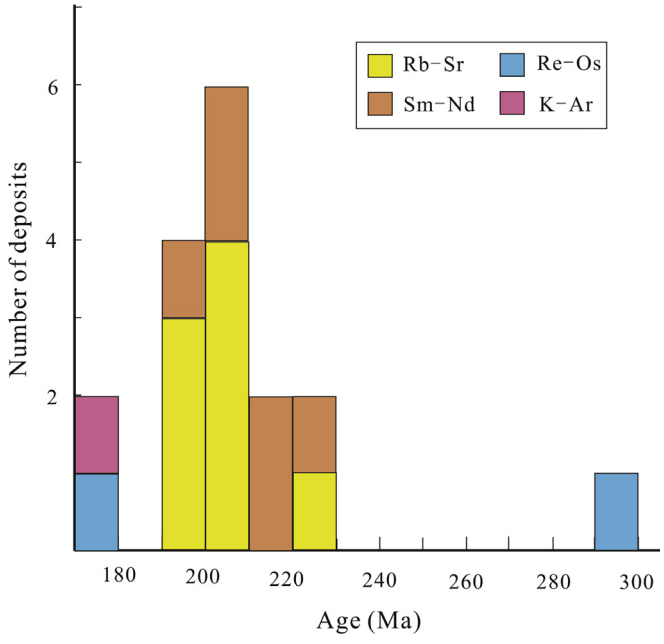

Fig. 22. A histogram of mineralization ages of deposits in the Sichuan-Yunnan-Guizhou Pb-Zn province (data from W.B. Li et al., 2004; C.Q. Zhang et al., 2005; Zhou et al., 2013c, 2015).

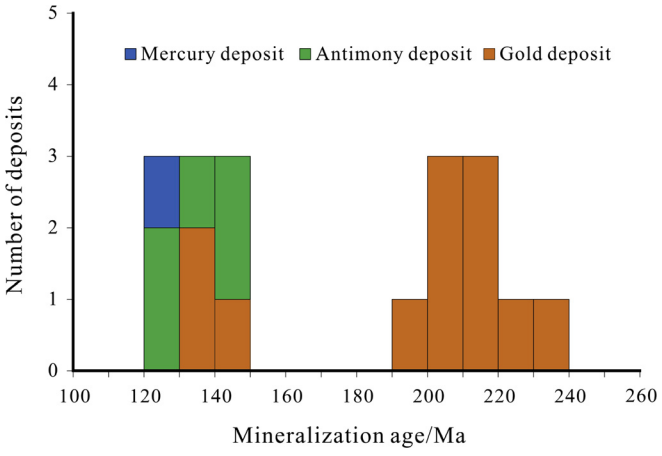

Fig. 23. A summary of reliable ages for gold, antimony and mercury deposits in the Youjiang Hu-As-Sb-Hg province (data from Peng et al., 2003b; Chen et al., 2009, 2015; Su et al., 2009b; Wang, 2013; Xiao, 2014; Wang and Wen, 2015; Pi et al., 2016).

ages of 126.4 ± 2.7 Ma and 128.2 ± 3.2 Ma for calcite from two veins in the Banian Sb deposit, and Xiao (2014) acquired a Sm-Nd isochron age of 130.5 ± 3 Ma for calcite from the Banpo Sb deposit. Wang and Wen (2015) reported a Sm-Nd isochron age of 129 ± 20 Ma for calcite from the Jiaoli-La'e Hg deposit.

The ages of the Au, Sb and Hg deposits in the Youjiang province mainly plot in two groups; ca. 130–150 Ma and 200–230 Ma (Fig. 23), implying two episodes of low-temperature metallogenesis. The Au mineralization probably formed dominantly during the 200-to-230-Ma period, whereas the Sb and Hg mineralization probably formed between 130 and 150 Ma, corresponding, to the Mesozoic Indosinian and Yanshanian events respectively. However, the late episode of mineralization may have overprinted the earlier one in some deposits, such as the Shuiyindong gold deposit (Su et al., 2009a; Chen et al., 2015).

6.3. Xiangzhong Sb-Au province

Previous studies of the ages of the deposits in the Xiangzhong Sb-Au province indicate there might have been two episodes of mineralization there as well. The Sb-Au deposits hosted in the basement metamorphic rocks mostly developed between 200 and 210 Ma. Li et al. (2008) reported Rb-Sr isochron ages of 205.6 ± 9.4 Ma and 204.8 ± 6.3 Ma for fluid inclusions trapped in quartz from the Chanziping and Daping gold deposits, whereas. Yao and Zhu (1993), Xiao et al. (1992) and Peng and Hu (2001b) obtained ages of the Fuzhuxi Sb-Au, Liaojiaping Sb-Au and Banxi Sb deposits of ca. 209 Ma, 200 Ma and 194–204 Ma, respectively.

The Sb deposits hosted in the carbonate cover rocks, such as the Xikuangshan giant Sb deposit, were probably formed mainly at 160–150 Ma. Hu et al. (1996) and Peng et al. (2003a) reported Sm-Nd isochron ages of 156.3 ± 12 Ma and 155.5 ± 1.1 Ma, respectively, for calcite from this deposit.

The Sb-Au deposits were formed at 200–210 Ma, mostly at the margin of the Xiangzhong Basin, where they are spatially related to Indosinian granitic intrusions. In contrast, the Sb deposits with ages of 150–160 Ma are mostly within the basin where no exposed granitic bodies are recognized.

In summary, the low-temperature ore deposits in the LTMD formed in two episodes, i.e. around 200–230 Ma and 130–160 Ma, corresponding to Indosinian (Triassic) and Yanshanian (Jurassic to Cretaceous) orogenies, respectively. The Indosinian metallogeny is recognized in three provinces, including Pb-Zn deposits in the Chua-Dian-Qian Pb-Zn province, the Carlin-type Au deposits in the Youjiang Au-As-Sb-Hg province and the Sb-Au deposits in the Xiangzhong province. However, Yanshanian metallogenesis occurred only in the Youjiang Au-As-Sb-Hg and Xiangzhong Sb-Au provinces, including the Sb and Hg deposits in the Youjiang province, and the Sb deposits in the Xiangzhong province. These two episodes of low-temperature metallogeny are consistent with those of granite-related W-Sn polymetallic deposits in the Cathaysia Block (Hu and Zhou, 2012; Mao et al., 2013).

7. A new geodynamic model for the South China metallogenic domain

It is now clear that the South China Craton was amalgamated in the early Neoproterozoic by collision of the Yangtze and Cathaysia Blocks and has since been modified by middle Paleozoic (Kwangsian), Triassic (Indosinian) and Jurassic-Cretaceous (Yanshanian) tectonothermal events (e.g., Charvet et al., 1996; Li, 1998; Li et al., 2009; Zhou et al., 2009; C.Q. Zhang et al., 2014; Wang et al., 2005, 2007a, 2007b; Y.J. Wang et al., 2010a,b, 2013; C.Q. Wang et al., 2012). The Indosinian event is commonly considered to have been responsible for the current tectonic framework of southern Asia through its accretion of the South China Craton to Eurasia (e.g., Huang et al., 1987; Ren, 1991; Qiu et al., 2016).

Initiation of Indosinian subduction of Indochina beneath the South China Craton is recorded by the 267–262-Ma magmatic arc in Hainan Island (X.H. Li et al., 2006), and the resulting plate convergence led to collision along the Song Ma suture zone at 258–243 Ma (Lepvrier et al., 1997; Carter et al., 2001; Maluski et al., 2005; Peng et al., 2006; Cai and Zhang, 2009; Y.J. Wang et al., 2010a,b). A Triassic intracontinental orogeny in South China is well documented (e.g., M.F. Zhou et al., 2006; X.M. Zhou et al., 2006; Wang et al., 2007a, 2013b). This orogeny resulted from the progressive closure of Paleotethys and subsequent collision between the South China Craton and the Indochina Block along the Song Ma suture to the south and between the North China Craton and the South China Craton along the Qinling-Dabie orogenic belt to the north. These two collisional events were accompanied by folding and thrusting of the strata, emplacement of abundant granitic plutons and widespread metamorphism. The southwestern margin of the South China Craton experienced substantial shortening during the continental collision (Wang et al., 2005, 2007b). The E–W-trending folds in the LTMD are the result of N-S compression during the Indosinian orogeny (Xu et al., 1992). Triassic peraluminous granites with ages from 258 to 205 Ma crop out in an area of about 14,000 km^2 in the South China Craton (Fig. 1) and are mainly distributed along E-W-trending faults as a result of the Indosinian event (X.M. Zhou et al., 2006). X.M. Zhou et al. (2006) proposed that the Early-Mid Triassic granites are intruded in syn-collisional compressional setting, whereas the Mid-Late Triassic granites are thought to be formed in post-collisional or syn-collisional extensional background (Qiu et al., 2014). The Mid-Late Triassic granites (ca. 230–200 Ma) are significantly later than the Indosinian Orogeny and its associated regional metamorphism (ca. 258–243 Ma), suggesting an extensional tectonic setting due to roll-back of the plate (Qiu et al., 2014). Decompressional partial melting triggered by roll-back extension was responsible for the origin of the Mid-Late Triassic granites (Qiu et al., 2014).

As already documented, the Chuan-Dian-Qian Pb-Zn metallogenic province was formed from basinal brine fluids, whereas the Youjiang Au-As-Sb-Hg and Xiangzhong Sb-Au provinces most probably resulted from mixed magmatic-meteoric fluids, although ore-forming elements of all deposits in the LTMD were dominantly from the sedimentary rocks. Combined with the ore-forming ages of ca. 200–230 Ma, a new geodynamic model is proposed for formation of the Indosinian metallogeny (Fig. 24).

The LTMD, especially the Youjiang and Chuan-Dian-Qian provinces, are located in the southwestern Yangtze Block, geographically far from the coastal area of South China, but near the Song Ma suture. In the Triassic, the Indosinian orogeny, related to collision of the Indochina Block with South China Block, triggered circulation of basinal brine fluids, which leached the ore-forming elements from the sedimentary strata to form the Chuan-Dian-Qian Pb-Zn province. There may be some buried Indosinian granitic intrusions in the Youjiang and Xiangzhong provinces as evidenced by geophysical investigations (Zhou, 1993; Li, 1996; Rao et al., 1999). These may have also triggered circulation of possibly meteoric fluids that leached the ore-forming elements from sedimentary strata to form the Carlin-type Au deposits in the Youjiang Au-As-Sb-Hg province, and the Sb-Au deposits in the Xiangzhong Sb-Au province.

The Indosinian orogeny was the main driving force for the widespread mineralization of the LTMD. Each of the three metallogenic provinces possesses unique features. The different styles of mineralization are believed to be due to the different geology of these three provinces (J.X. Zhou et al., 2014; M.F. Zhou et al., 2014). The eastern part of the Yangtze Block is known as the Jiangnan orogeny with the Neoproterozoic Sibao Group (830–815 Ma)

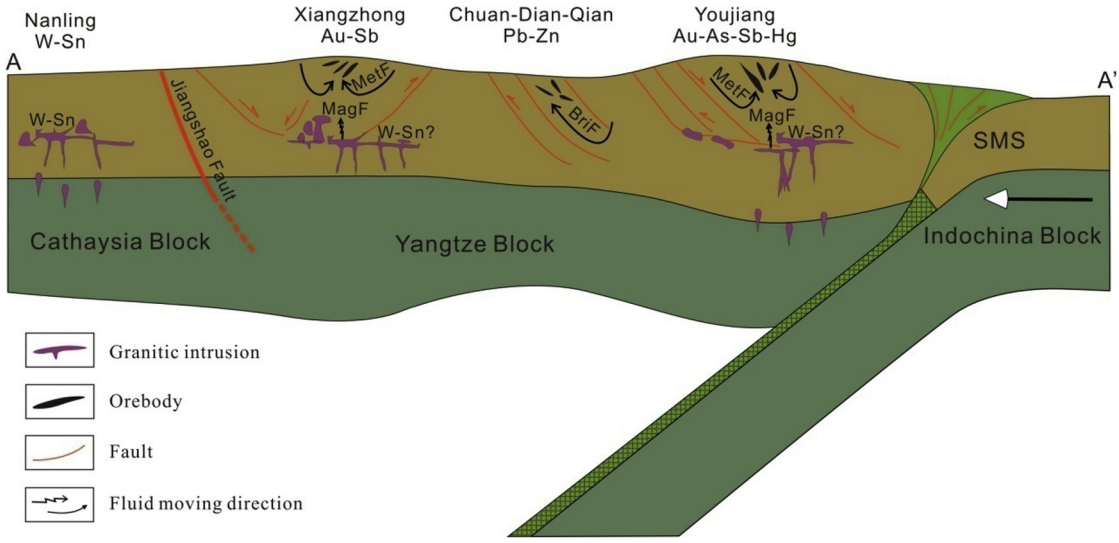

Fig. 24. A proposed metallogenic model for the South China LTMD related to the Indosinian syn-collisional extension. The geodynamic setting is modified after Qiu et al. (2014). BriF-Brine Fluid; MagF-Magmatic Fluid; MetF-Meteoric Fluid; SMS-Song Ma Suture.

and Banxi Group (800–730 Ma), whereas there are widespread Paleoproterozoic (~1.7 Ga) and Mesoproterozic strata (~1.0 Ga).

The Yanshanian event in the South China Craton was dominantly represented by the development of I-, S- and A-type granites in the Cathaysia Block (e.g. Zhao et al., 2015). The associated deposits were petrogenetically related to input of juvenile, mantle-derived magmas in response to an extensional regime in the entire South China Craton. These igneous rocks were formed in three stages; 152–180 Ma (peak at 158 Ma), 120–130 Ma (peak at 125 Ma) and 87–107 Ma (peak at 93 Ma) but most formed at ca. 158 Ma (Y.J. Wang et al., 2012). Recent dating results indicate an ore-forming age of ca. 150 Ma for Sb deposits in the Xiangzhong province and for Hg and Sb deposits in the Youjiang province, coinciding with the age of Jurassic magmatism in the South China Craton. This observation suggests that the Yanshanian metallogeny overprinted the Youjiang and Xiangzhong provinces during development of the Jurassic magmatism.

It should be noted that, as the metallogenic episodes of low-temperature deposits in the Youjiang and Xiangzhong provinces are temporally consistent with those of granite-related W-Sn polymetallic deposits in the Cathaysia Block (Hu and Zhou, 2012; Mao et al., 2013), there might be some buried granite-related W-Sn mineralization beneath these two provinces where the formation of low-temperatue deposits were also triggered by the simultaneous deep-seated granitic magmatism (Fig. 24).

8. Conclusions

(1) The South China low-temperature metallogenic domain extends over an area of around 500,000 km^2 in the Yangtze Block and includes the Chuan-Dian-Qian Pb-Zn, Youjiang Au-As-Sb-Hg and Xiangzhong Sb-Au metallogenic provinces.
(2) Ore deposits in the three provinces formed mostly at 200–230 Ma, corresponding to the Indosinian orogeny. Those in the Youjiang and Xiangzhong provinces were overprinted by the Yanshanian orogeny.
(3) The ages of low-temperature ore deposits in the LTMD are similar to those of granite-related, W-Sn deposits in the Cathaysia Block, implying a similar geodynamic setting.
(4) The Indosinian orogeny, followed by collision of the Indochina Block with the South China Craton, triggered circulation of basinal brine fluids that leached the ore-forming elements from sedimentary rocks to form the Chuan-Dian-Qian Pb-Zn province. Deep-seated granitic magmas, formed during the Indosinian orogeny, triggered circulation of possibly meteoric fluids, which also leached ore-forming elements from sedimentary rocks to form the Carlin-type Au deposits in the Youjiang province, and the Sb-Au deposits in the Xiangzhong province.
(5) The *Indosinian* intracontinental orogeny established the ore-forming framework of the LTMD. The Yanshanian metallogeny overprinted deposits in the Youjiang and Xiangzhong provinces due to development of Jurassic magmatism, in a fashion similar to that of the Indosinian metallogeny in these two provinces.

Acknowledgements

This research was supported jointly by the National "973" Program of China (2014CB440906), the Key project of the National Natural Science Foundation of China (41230316), and the CAS/SAFEA International Partnership Program (KZZD-EW-TZ-20). The manuscript benefitted from thoughtful reviews by Prof. Paul Robinson and Prof. Danping Yan, to whom we are grateful.

References

Arehart, G.B., Chakurian, A.M., Tertbar, D.R., Christensen, J.N., McInnes, B.I.A., Donelick, R.A., 2003. Evaluation of radioisotope dating of Carlin-type deposits in the Great Basin, Western North America, and Implications for Deposit Genesis. Econ. Geol. 2, 235–248.
Bai, D.Y., Jia, B.H., Wang, X.H., Peng, Y.Y., Jia, P.Y., Ling, Y.X., 2013. Kinematics of tectonic deformation of the western Xiangzhong Basin and its tectonic mechanism. Acta Geol. Sin. 87, 1791–1802 (in Chinese with English abstract).
BGMRHN (Bureau of Geology and Mineral Resources of Hunan Province), 1988. Regional Geology of the Hunan Province. Geological Publishing House, Beijing, pp. 286–507 (in Chinese with English summary).
Cai, J.X., Zhang, K.J., 2009. A new model for the Indochina and South China collision during the Late Permian to the Middle Triassic. Tectonophysics 469, 35–45.
Cao, L., Duan, Q.F., Peng, S.G., Zhou, Y., 2015. Characteristics of fluid inclusions in the Chanziping gold deposit in Xuefeng Mountains and their geological implications. Geol. Explor. 51, 212–224 (in Chinese with English abstract).
Cao, Y.J., Li, J., Chen, F., Wang, C.J., Liu, B.D., 2014. On geological characteristics and ore prospecting indicators of Chanziping gold deposit in Hunan. J. Geol. 38, 309–313 (in Chinese with English abstract).
Carter, A., Roques, D., Bristow, C., Kinny, P., 2001. Understanding Mesozoic accretion in Southeast Asia: significance of Triassic thermotectonism (Indosinian orogeny) in Vietnam. Geology 29, 211–214.

Charvet, J., Shu, L.S., Faure, M., Choulet, F., Wang, B., Lu, H.F., Breton, N.L., 2010. Structural development of the Lower Paleozoic belt of South China: genesis of an intracontinental orogen. J. Asian Earth Sci. 39, 309–330.
Charvet, J., Shu, L.S., Shi, Y.S., Guo, L.Z., Faure, M., 1996. The building of south China: collision of Yangtze and Cathaysia blocks, problems and tentative answers. J. SE Asian Earth Sci. 13, 223–235.
Chaussidon, M., Albarède, F., Sheppard, S.M., 1989. Sulphur isotope variations in the mantle from ion microprobe analyses of micro-sulphide inclusions. Earth Planet. Sci. Lett. 92, 144–156.
Chen, D., Wu, L.F., 2012. Distribution and metallogeny of Pb-Zn deposits in the Sichuan-Yunnan-Guizhou border region. J. Sichuan Geol. 32, 304–308 (in Chinese with English abstract).
Chen, D.Y., Zou, Z.X., 2000. Studying situation about Lanmuchang type Thallium (mercury) Ore deposits in Southwestern Guizhou. Guizhou Geol. 17, 236–241 (in Chinese with English abstract).
Chen, J., Han, R.S., Gao, D.R., Zhao, D.S., 2001. Geological characteristics of Huize Pb-Zn deposit, Yunnan and model of ore-prospecting method. Geol.-Geochem. 29, 124–129 (in Chinese with English abstract).
Chen, J.F., Jahn, B., 1998. Crustal evolution of southeastern China: Nd and Sr isotopic evidence. Tectonophysics 284, 101–133.
Chen, C.H., Hsieh, P.S., Lee, C.Y., Zhou, H.W., 2011. Two episodes of the Indosinian thermal event on the South China Block: constraints from LA-ICPMS U-Pb zircon and electron microprobe monazite ages of the Darongshan S-type granite suite. Gondwana Res. 19, 1008–1023.
Chen, C.H., Lee, C.Y., Shinjo, r., 2016. The epilog of the western paleo-Pacific subduction: inferred from spatial and temporal variations and geochemistry of the Late Cretaceous to Early Cenozoic silicic magmatism in coastal South China. J. Asian Earth Sci. 115, 520–546.
Chen, M.H., 2007. The genetic model of Jinfeng (Lannigou) gold deposit based on the coupling of metallotectonics and ore-forming fluid (PhD thesis). Chinese Academy of Geological Sciences, Beijing, pp. 1–233 (in Chinese with English abstract).
Chen, M.H., Huang, Q.W., Hu, Y., Chen, Z.Y., Zhang, W., 2009. Genetic types of phyllosilicate (micas) and its ^{39}Ar–^{40}Ar dating in Lannigou gold deposit, Guizhou Province, China. Acta Mineral. Sin. 29, 353–362 (in Chinese with English abstract).
Chen, M.H., Zhang, Y., Meng, Y.Y., Lu, G., Liu, S.Q., 2014a. The confirmation of the upper limit of metallogenetic epoch of Liaotun gold deposit in western Guangxi, China, and its implication on chronology of Carlin-type gold deposits in Yunnan–Guizhou–Guangxi "golden triangle" area. Mineral Deposits 33, 1–13 (in Chinese with English abstract).
Chen, M.H., Mao, J.W., Bierlein, F.P., Norman, T., Uttley, P.J., 2011. Structural features and metallogenesis of the Carlin-type Jinfeng (Lannigou) gold deposit, Guizhou Province, China. Ore Geol. Rev. 43, 217–234.
Chen, M.H., Zhang, Z.Q., Santosh, M., Dang, Y., Zhang, W., 2014b. The Carlin-type gold deposits of the "golden triangle" of SW China: Pb and S isotopic constraints for the ore genesis. J. Asian Earth Sci. 103, 115–128.
Chen, M.H., Mao, J.W., Li, C., Zhang, Z.Q., Dang, Y., 2015. Re–Os isochron ages for arsenopyrite from Carlin-like gold deposits in the Yunnan–Guizhou–Guangxi "golden triangle", southwestern China. Ore Geol. Rev. 64, 316–327.
Chen, S.M., 2012. Research of multiple geosciences information prospecting prediction in Xikuangshan antimony ore field PhD thesis. China University of Geosciences, Beijing, pp. 1–306 (in Chinese with English abstract).
Chen, X.L., Jiang, Y.H., Li, S.Y., Liao, H.Z., 1983. A preliminary study on the origin of the Xikuangshan antimony deposits in Hunan. Geol. Rev. 5, 486–493 (in Chinese with English abstract).
Chen, Y.C., 2001. Gold Deposits in China and the Metallogenic Regularity. Geological Publishing House, Beijing, pp. 1–465 (in Chinese with English abstract).
Cheng, Y.S., 2013. Geology and sulfur isotope geochemistry of Dafulou tin-polymetallic deposit in Dachang ore field, Guangxi, China. J. Central South Univ. 20, 2811–2818 (in Chinese with English abstract).
Chu, Y., Faure, M., Lin, W., Wang, Q.C., Ji, W.B., 2012a. Tectonics of the Middle Triassic intracontinental Xuefengshan Belt, South China: new insights from structural and chronological constraints on the basal decollement zone. Int. J. Earth Sci. 101, 2125–2150.
Chu, Y., Lin, W., Faure, M., Wang, Q.C., Ji, W.B., 2012b. Phanerozoic tectonothermal events of the Xuefengshan Belt, central South China: implications from U-Pb age and Lu-Hf determinations of granites. Lithos 150, 243–255.
Cui, S., Li, J., 1983. On the Indosinian orogeny along the Chinese Western Pacific belt. Acta Geol. Sin. 57, 51–61 (in Chinese with English abstract).
Dai, C.H., 2000a. Deposit-controlled characteristics of NW-trending structure and prospecting significance about Au ores zone of Gutaishan-Gaojia'ao. Hunan Geol. 19, 105–110 (in Chinese with English abstract).
Dai, C.H., 2000b. The geological feature of Qingjingzhai gold deposit of Xinhua County and the meaning of conducting ore-prospecting there. Gold 21, 8–10 (in Chinese with English abstract).
Dai, H.Z., Chen, C.H., Gu, X.X., Li, B.H., Dong, S.Y., Cheng, W.B., 2014. Characteristics of ore-forming fluids from zhesang gold deposit in Funing County, Yunnan Province. Geoscience 28, 893–904 (in Chinese with English abstract).
Deng, F., 2009. The geological characteristics and elemental geochemistry research about Xingren Lanmuchang thallium Master thesis. Kunming University of Science and Technology, Kunming, pp. 1–76 (in Chinese with English abstract).
Dong, L., Huang, J.G., Li, W.J., 2011. Geological characteristics and origin of Getang gold deposits in Guizhou. J. Southwest Univ. Sci. Technol. 26, 41–44 (in Chinese with English abstract).
Fan, D.L., Zhang, T., Ye, J., 2004. The Xikuangshan Sb deposit hosted by the Upper Devonian black shale series, Hunan, China. Ore Geol. Rev. 24, 121–133.
Fan, W.M., Zhang, C.H., Wang, Y.J., Guo, F., Peng, T.P., 2008. Geochronology and geochemistry of Permian basalts in western Guangxi Province, Southwest China: evidence for plume-lithosphere interaction. Lithos 102, 218–236.
Faure, M., Ishida, K., 1990. The Mid-Upper Jurassic olistostrome of the west Philippines: a distinctive key-marker for the North Palawan block. J. SE Asian Earth Sci. 4, 61–67.
Faure, M., Lepvrier, C., Nguyen, V.V., Vu, T.V., Lin, W., Chen, Z., 2014. The South China block-Indochina collision: where, when, and how? J. Asian Earth Sci. 79, 260–274.
Faure, M., Shu, L.S., Wang, B., Charvet, J., Choulet, F., Monié, P., 2009. Intracontinental subduction: a possible mechanism for the Early Paleozoic Orogen of SE China. Terra Nova 21, 360–368.
Feng, C.Y., Zeng, Z.L., Zhang, D.Q., Qu, W.J., Du, A.D., Li, D.X., She, H.Q., 2011. SHRIMP zircon U-Pb and molybdenite Re–Os isotopic dating of the tungsten deposits in the Tianmenshan-Hongtaoling W-Sn orefield, southern Jiangxi Province, China, and geological implications. Ore Geol. Rev. 43, 8–25.
Fu, S.H., 2004. Metallogenesis of Pb-Zn deposits and enrichment regularity of dispersed elements Cd, Ga, and Ge in SW Yangtze block PhD thesis. Institute of Geochemistry, Chinese Academy of Sciences, Guiyang, pp. 1–92 (in Chinese with English abstract).
Galfetti, T., Bucher, H., Martini, R., Hochuli, P.A., Weissert, H., Crasquin-Soleau, S., Brayard, A., Goudemand, N., Brühwiler, T., Kuang, G.D., 2008. Evolution of Early Triassic outer platform paleoenvironments in the Nanpanjiang Basin (South China) and their significance for the biotic recovery. Sed. Geol. 204, 36–60.
Gilder, S.A., Gill, J., Coe, R.S., 1996. Isotopic and paleomagnetic constraints on the Mesozoic tectonic evolution of south China. J. Geophys. Res.-Solid Earth 101, 16137–16154.
Gong, G.L., Chen, G.H., Dai, J.B., Chen, X., Li, W.Y., 2007. Tectono-controlling characteristics and genesis of Daxin gold deposit in Hunan province. Geotect. Metall. 3, 342–347 (in Chinese with English abstract).
Gu, X.X., Zhang, Y.M., Li, B.H., Dong, S.Y., Xue, C.J., Fu, S.H., 2012. Hydrocarbon and ore-bearing basinal fluids: a possible link between gold mineralization and hydrocarbon accumulation in the Youjiang basin, South China. Mineral. Deposit 47, 663–682.
Guo, X., 2007. Ore-forming characteristics of the Jinshachang Pb-Zn deposit and the perspective prediction of its deep part and periphery, Northeast Yunnan. Mineral Resour. Geol. 21, 636–641 (in Chinese with English abstract).
Han, R.S., Chen, J., Li, Y., Ma, D.Y., Zhao, D.S., Ma, G.S., 2001. Ore-controlling tectonics and prognosis of concealed ore in Huize Pb-Zn deposit, Yunnan. Acta Mineral. Sin. 21, 265–269 (in Chinese with English abstract).
Han, R.S., Hu, Y.Z., Wang, X.K., Hou, B.H., Huang, Z.L., Chen, J., Wang, F., Wu, P., Li, B., Wang, H.J., Dong, Y., Lei, L., 2012. Mineralization model of rich-Ge-Ag-bearing Zn-Pb polymetallic deposit concentrated district in northeastern Yunnan, China. Acta Geol. Sin. 86, 280–294 (in Chinese with English abstract).
Han, R.S., Zou, H.J., Hu, B., Hu, Y.Z., Xue, C.D., 2007. Features of fluid inclusions and sources of ore-forming fluid in the Maoping carbonate-hosted Zn-Pb-(Ag-Ge) deposit, Yunnan, China. Acta Petrol. Sin. 23, 2109–2118 (in Chinese with English abstract).
He, M.Y., Lou, Y.E., Wang, P., 2002. Relationship between silicification and stibnite mineralization in Xikuangshan antimony deposit, Hunan Province. Mineral Deposits 21, 384–387 (in Chinese with English abstract).
He, S.H., Rong, H.F., Shang, W., Su, J.H., 2006. Geological characteristics and genesis of Maozu lead and zinc deposit, Yunnan. Mineral Resour. Geol. 20, 397–402 (in Chinese with English abstract).
Hofstra, A., Emsbo, P., Christiansen, W., Theodorakos, P., Zhang, X.C., Hu, R.Z., Su, W. C., Fu, S.H., 2005. Source of ore fluids in Carlin-type gold deposits, China: Implications for genetic models. In: Proceedings Mineral Deposit Research. Meeting the Global Challenge. Springer, pp. 533–536.
Hou, L., Peng, H.J., Ding, J., Zhang, J.R., Zhu, S.B., Wu, S.Y., Wu, Y., Ouyang, H.G., 2016. Textures and in situ chemical and isotopic analyses of pyrite, Huijiabao Trend, Youjiang Basin, China: implications for paragenesis and source of sulfur. Econ. Geol. 111, 331–353.
Hu, C.N., 1991. Geologic feature and metallotectonic analysis of Banxi antimony ore deposit, Taojiang County. Hunan Geol. 10, 317–321 (in Chinese with English abstract).
Hu, R.Z., Mao, J.W., Hua, R.M., Fan, W.M., 2015. Intra-Continental Mineralization of South China Craton. Science Press, Beijing, pp. 1–903 (in Chinese).
Hu, R.Z., Su, W.C., Bi, X.W., Tu, G.Z., Hofstra, A.H., 2002. Geology and geochemistry of Carlin-type gold deposits in China. Mineral. Deposita 37, 378–392.
Hu, R.Z., Peng, J.T., Ma, D.S., Su, W.C., Shi, C.H., Bi, X.W., Tu, G.Z., 2007. Epoch of large-scale low-temperature mineralization in southwestern Yangtze massif. Mineral Deposits 26, 583–596 (in Chinese with English abstract).
Hu, R.Z., Zhou, M.F., 2012. Multiple Mesozoic mineralization events in South China-an introduction to the thematic issue. Mineral. Deposita 47, 579–588.
Hu, X.W., Pei, R.F., Zhou, S., 1996. Sm-Nd dating for antimony mineralization in the Xikuangshan deposit, Hunan, China. Resour. Geol. 4, 227–231.
Hua, Y.F., Cui, M.Z., 1996. A genetic model f or the Wanshan superlarge mercury deposit, Guizhou. Guizhou Geol. 13, 161–165 (in Chinese with English abstract).
Huang, J.G., Li, H.J., Li, W.J., Dong, L., 2012a. Trace element characteristics of fluorite and its Sm-Nd isotopic dating in Getang gold deposit, Guizhou Province. Adv. Earth Sci. 27, 1087–1093 (in Chinese with English abstract).
Huang, J.G., Li, H.J., Li, W.J., Dong, L., 2012b. Element geochemistry of ore-bearing rock series in the Getang gold deposit, Guizhou Province. Geol. China 39, 1318–1326 (in Chinese with English abstract).

Huang, J.Q., Ren, J.S., Jiang, C.F., Zhang, Z.K., Qin, D.Y., 1987. Geotectonic Evolution of China. Springer-Verlag, Berlin, pp. 1–203.
Jiang, Z.Y., Wei, L.M., Chen, M.Y., 1990. Sulfur isotopic study of sulfides from sedimentary strata and strata-bound deposits in Hunan, Guangdong and Guangxi of Southern China. Geochemica 19, 117–126 (in Chinese with English abstract).
Jin, J.F., Tao, Y., Zeng, L.J., 2001. The ore-forming fluid of Xikuangshan-type antimony deposits. Bull. Mineral., Petrol. Geochem. 3, 156–164 (in Chinese with English abstract).
Jin, J.F., 2002. Locating mechanism of superlarge antimony deposit—Xikuangshan antimony deposit example. Bull. Mineral., Petrol. Geochem. 3, 145–151 (in Chinese with English abstract).
Kang, R.H., 2001. Geo-geochemical gold prospecting model for the Gaojia'ao gold deposit, the middle part of Hunan. Gold Geol. 7, 59–63 (in Chinese with English abstract).
Kuang, W.L., 2000. Research on the metallogenic model of Xikuangshan superlarge antimony deposit. World Geol. 19, 26–30 (in Chinese with English abstract).
Lepvrier, C., Maluski, H., Van Vuong, N., Rogues, D., Axente, V., Rangin, C., 1997. Indosinian NW-trending shear zones within the Truong Son belt (Vietnam) ^{40}Ar-^{39}Ar Triassic ages and Cretaceous to Cenozoic overprints. Tectonophysics 283, 105–127.
Lepvrier, C., Maluski, H., Vu, V.T., Leyreloup, A., Phan, T.T., Nguyen, V.V., 2004. The Early Triassic Indosinian Orogeny in Vietnam (Truong Son Belt and Kontum Massif): implications for the geodynamic evolution of Indochina. Tectonophysics 393, 87–118.
Li, C.Y., 1999. Some geological characteristics of concentrated distribution area of epithermal deposits in China. Earth Sci. Front. 6, 163–170 (in Chinese with English abstract).
Li, F.S., Kang, R.H., Chen, Y.W., Wu, Y.C., Yuan, W., 2002. The metallogenic geological condition of Gaojia'ao Hunan province and its ore-prospecting orientation. Gold 22, 1–3 (in Chinese with English abstract).
Li, F.Y., Gu, X.X., Fu, S.H., Zhang, M., 2003. Dating methods for MVT Pb-Zn deposits: a review. Contrib. Geol. Mineral Resour. Res. 18, 163–167.
Li, H.Q., Wang, D.H., Chen, F.W., Mei, Y.P., Cai, H., 2008. Study on chronology of the Chanziping and Daping gold deposit in Xuefeng Mountain, Hunan province. Acta Geol. Sin. 7, 900–905 (in Chinese with English abstract).
Li, H.T., Cao, D.Y., Wang, L.J., Guo, A.J., Li, Y.F., Xu, H., 2013. Characteristics and evolution of coal-controlled structures on the east slope of the Xuefengshan domain in central Hunan Province. Geotect. Metall. 37, 611–621 (in Chinese with English abstract).
Li, J.H., 2007. The geological characteristics of Daxin gold deposit of Xinshao County of Hunan. Gold Sci. Technol. 15, 8–12 (in Chinese with English abstract).
Li, J.H., Wu, J.C., Zhou, Y.J., 2004. Ore-control rules of dome structure in Baimashan-Co-Longshan gold belt, Central Hunan. Gold Geol. 10, 32–36 (in Chinese with English abstract).
Li, S.S., 1996. Evolution of antimony mineralization by the mantle plume of deep fluid in central Hunan. Hunan Geol. 15, 137–142 (in Chinese with English abstract).
Li, W.B., Huang, Z.L., Wang, Y.X., Chen, J., Han, R.S., Xu, C., Guan, T., Yin, M.D., 2004. Age of the giant Huize Zn-Pb deposits determined by Sm-Nd dating of hydrothermal calcite. Geol. Rev. 78, 507–518 (in Chinese with English abstract).
Li, X.B., Huang, Z.L., Li, W.B., Zhang, Z.L., Yan, Z.F., 2006a. Sulfur isotopic compositions of the Huize super-large Pb-Zn deposit, Yunnan Province, China: implications for the source of sulfur in the ore-forming fluids. J. Geochem. Explor. 89, 227–230.
Li, X.H., Li, Z.X., Li, W.X., Wang, Y.J., 2006b. Initiation of the Indosinian Orogeny in South China: evidence for a Permian magmatic arc on the Hainan Island. J. Geol. 114, 341–353.
Li, X.H., 2000. Cretaceous magmatism and lithospheric extension in Southeast China. J. Asian Earth Sci. 18, 293–305.
Li, X.H., Li, W.X., Li, Z.X., Lo, C.H., Wang, J., Ye, M.F., Yang, Y.H., 2009. Amalgamation between the Yangtze and Cathaysia Blocks in South China: Constraints from SHRIMP U-Pb zircon ages, geochemistry and Nd–Hf isotopes of the Shuangxiwu volcanic rocks. Precambr. Res. 174, 117–128.
Li, Z.X., 1998. Tectonic history of the major East Asian lithospheric blocks since the mid-Proterozoic: a synthesis. In: Flower, M.F.J., Chung, S.L., Lo, C.H., Lee, C.Y. (Eds.), Mantle Dynamics and Plate Interactions in East Asia, vol. 27. American Geophysical Union, pp. 221–243 (Geodynamic series).
Li, Z.X., Li, X.H., 2007. Formation of the 1300-km-wide intracontinent orogen and post-orogenic magmatic province in Mesozoic South China. Geology 35, 179–182.
Liang, G.B., Huang, T.X., Hu, M.A., Yang, Z., 2015. Electron microprobe analysis on gold-bearing mineralsfrom Mingshan gold deposit in northwest Guangxi. J. Guilin Univ. Technol. 35, 236–242 (in Chinese with English abstract).
Liang, H.Y., 1991. Geochemistry of ore fluid and genesis of Longshan Au-Sb deposits, west Hunan, China. Geochemica 4, 342–350 (in Chinese with English abstract).
Lin, F.M., 2014. On the ore-forming fluid in the Xikuangshan antimony deposit, central Hunan Master thesis. Center South University, Changsha, pp. 1–62 (in Chinese with English abstract).
Lin, Z.Y., Wang, D.H., Zhang, C.Q., 2010. Rb–Sr isotopic age of sphalerite from the Paoma lead-zinc deposit in Sichuan Province and its implications. Geol. China 37, 488–494 (in Chinese with English abstract).
Liu, H., 2013. Study on geochemical characteristics and ore-searching prospecting of Jinya gold deposit, Northwestern of Guangxi Master thesis. Guangxi University, Nanchang, pp. 1–67 (in Chinese with English abstract).
Liu, H.C., 1996. Pb-Zn source beds (rocks) of Dian-Chuan-Qian metallogenic region. Geol. Explor. 32, 12–18 (in Chinese with English abstract).
Liu, H.P., Zhang, Y.L., Hu, W.Q., 1985. A discussion on ore genesis of the Xikuangshan Sb deposit in Hunan. Hunan Geol. 1, 28–39 (in Chinese with English abstract).
Liu, J.Z., Chen, J.H., Deng, Y.M., Fu, Z.K., Chen, F.E., Chen, M., You, B., 2009. Exploration of the Shuiyindong super-scale gold deposit and the evolution of exploration for metallogenic belt of the Huijiabao anticline in Guizhou Province. Geol. Survey Res. 32, 138–143 (in Chinese with English abstract).
Liu, J.Z., Deng, Y.M., Liu, C.Q., Zhang, X.C., Xia, Y., 2006. Metallogenic conditions and model of the superlarge Shuiyindong stratabound gold deposit in Zhenfeng County, Guizhou Province. Geol. China 33, 169–177 (in Chinese with English abstract).
Liu, L., Gu, X.X., Peng, Y.W., Zhang, Y.M., Wu, C.Y., Cheng, W.B., 2012. Characteristics of fluid inclusions and fluid immiscibility mechanism of the Taipingdong gold deposit, Guizhou. Acta Petrol. Sin. 28, 1568–1576 (in Chinese with English abstract).
Liu, P., Li, P.G., Ma, R., Han, Z.H., Yang, G.L., Ye, D.S., 2006. A gold associated with pyroclastic rock and hydrothermal exhalation: nibao gold deposit in Guizhou Province, China. Mineral Deposits 25, 101–110 (in Chinese with English abstract).
Liu, P.C., Tang, Q.G., Li, H.C., 2008. Geological characteristics, enrichment laws and prospecting direction of gold-antimony deposit in Longshan deposits of Hunan. Geol. Prospect. 44, 31–38 (in Chinese with English abstract).
Liu, S., Su, W.C., Hu, R.Z., Feng, C.X., Gao, S., Coulson, I.M., Wang, T., Feng, G.Y., Tao, Y., Xia, Y., 2010. Geochronological and geochemical constraints on the petrogenesis of alkaline ultramafic dykes from southwest Guizhou Province, SW China. Lithos 114, 253–264.
Liu, S.Q., Chen, M.H., Yang, F., Dai, Y., Zhang, Y., 2014. Re-Os dating and sulfur isotope tracing of arsenopyrites from Jinya gold deposit in Guangxi. J. Guilin Univ. Technol. 34, 423–430 (in Chinese with English abstract).
Liu, W.J., 1992. Genesis of some antimony deposits in Southern China. J. Chengdu College Geol. 19, 10–19 (in Chinese with English abstract).
Liu, X.J., Liang, Q.D., Li, Z.L., Castillo, P.R., Shi, Y., Xu, J.F., Huang, X.L., Liao, S., Huang, W.L., Wu, W.N., 2016. Origin of Permian extremely high Ti/Y mafic lavas and dykes from Western Guangxi, SW China: implications for the Emeishan mantle plume magmatism. J. Asian Earth Sci. http://dx.doi.org/10.1016/j.jseaes.2016.09.005.
Liu, Y., 2015. Study of the nature of ore-forming fluids and metallogenic model of the Carlin-type gold deposits in the Youjiang Basin, China Ph.D. thesis (unpublished). Nanjing University, Nanjing (in Chinese with English abstract).
Liu, Z.H., 2005. Sedimentary facies differentiation and its mechanism during Permian in central-southern Hunan. Chin. J. Geol. 40, 510–517 (in Chinese with English abstract).
Lu, X.W., 1999. Regional ore-controlling characteristics of gold and antimony deposits in central Hunan. Uranium Geol. 15, 344–349 (in Chinese with English abstract).
Lu, X.W., Ma, D.S., Wang, W.Y., 2000. Geochemical characteristics of regional paleofluid of central Hunan. Contrib. Geol. Mineral Resour. Res. 15, 320–327 (in Chinese with English abstract).
Luo, G., Yang, X.F., 2010. Geological characteristics and metallogenic regularity of fine disseminated type gold deposit at Laozhaiwanin Guangnan area, Yunnan, China. Geol. Bull. China 29, 1362–1370 (in Chinese with English abstract).
Luo, X.L., 1995. Geological characteristics of the formation of Banxi antimony deposits in Hunan. J. Guilin Inst. Technol. 15, 231–242 (in Chinese with English abstract).
Ma, D.S., Pan, J.Y., Xie, Q.L., He, J., 2002. Ore source of Sb (Au) deposits in Center Hunan: I.Evidences of trace elements and experimental geochemistry. Mineral Deposits 3, 366–376 (in Chinese with English abstract).
Ma, D.S., Pan, J.Y., Xie, Q.L., 2003. Ore sources of Sb (Au) deposits in Center Hunan: II. Evidence of isotopic geochemistry. Mineral Deposits 21, 78–87 (in Chinese with English abstract).
Maluski, H., Lepvrier, C., Leyreloup, A., Tich, V.V., Thi, P.T., 2005. ^{40}Ar-^{39}Ar geochronology of the charnockites and granulites of the Kan Nack complex Kon Tum Massif, Vietnam. J. Asian Earth Sci. 25, 653–677.
Mao, J.W., Cheng, Y.B., Chen, M.H., Pirajno, F., 2013. Major types and time-space distribution of Mesozoic ore deposits in South China and their geodynamic settings. Mineral. Deposita 48, 267–294.
Murao, S., Sie, S.H., Hu, X., Suter, G.F., 1999. Contrasting distribution of trace elements between representative antimony deposits in southern China. Nucl. Instrum. Meth. Phys. Res. B 150, 502–509.
Nie, A.G., 2007. A mineralization mechanism as well as mineralogenetic prospect of Carlin-type gold deposit in southwestern of Guizhou PhD thesis. Kunming University of Science and Technology, Kunming, pp. 1–142 (in Chinese with English abstract).
Ohmoto, H., 1986. Stable isotopes in high temperature geological process. Rev. Mineral. Geochem., Mineral Soc. Am. 16, 491–559.
Ohmoto, H., Rye, R.O., 1979. Isotopes of sulfur and carbon. In: Barnes, H.L. (Ed.), Geochemistry of Hydrothermal Ore Deposits. second ed. Wiley, New York, pp. 509–567.
Pang, B.C., Yang, D.S., Zhou, Z., Liu, Y.M., Liu, P.C., Liu, Y.D., 2011. Trace elements in pyrites and their implication for hydrothermal ore-forming process in Longshan gold-antimony deposit, Hunan, China. Geoscience 25, 832–845 (in Chinese with English abstract).
Peng, J.T., Hu, A.X., Zhang, L.S., Lei, W.Y., Yang, J.H., Lin, F.M., 2014. Zircon U-Pb dating of the lamprophyre in the Xikuangshan mining district, central Hunan

and its geological implications. Geotect. Metall. 38, 686–693 (in Chinese with English abstract).
Peng, J.T., Hu, R.Z., 2001a. Carbon and oxygen isotope systematic in the Xikuangshan giant antimony, center Hunan. Geol. Rev. 1, 34–41 (in Chinese with English abstract).
Peng, J.T., Hu, R.Z., 2001b. Metallogenic epoch and metallogenic tectonic environment of antimony deposits, South China. Geol.-Geochem. 29, 104–108 (in Chinese with English abstract).
Peng, J.T., Hu, R.Z., Burnard, P.G., 2003a. Samarium-neodymium isotope systematics of hydrothermal calcite from the Xikuangshan antimony deposit (Hunan, China): the potential of calcite as a geochronometer. Chem. Geol. 200, 129–136.
Peng, J.T., Hu, R.Z., Jiang, G.H., 2003b. Samarium-neodymium isotope system of fluorites from the Qinglong antimony deposit, Guizhou Province: constraints on the mineralizing age and ore-forming minerals sources. Acta Petrol. Sin. 19, 785–791 (in Chinese with English abstract).
Peng, J.T., Hu, R.Z., Zou, L.Q., Liu, J.X., 2002. Isotopic tracing of ore-forming materials for Xikuangshan antimony deposit, center Hunan. Acta Mineral. Sin. 2, 155–159 (in Chinese with English abstract).
Peng, T.P., Wang, Y.J., Fan, W.M., Liu, D.Y., Shi, Y.R., Miao, L.C., 2006. The SHRIMP zircon U-Pb geochronology of the early Mesozoic felsic igneous rocks from the southern Langcangjiang and its tectonic implications. Sci. China (D) 49, 1032–1042.
Peng, Y.W., Gu, X.X., Zhang, Y.M., Liu, L., Wu, C.Y., Chen, S.Y., 2014. Ore-forming process of the Huijiabao gold district, southwestern Guizhou Province, China: evidence from fluid inclusions and stable isotopes. J. Asian Earth Sci. 2014 (93), 89–101.
Qin, L.J., Liu, D.M., 2006. Geochemical characteristics of the Taipingdong gold deposit, Xinren County, Guizhou. Guizhou Geol. 23, 187–192 (in Chinese with English abstract).
Qiu, L., Yan, D.P., Zhou, M.F., Arndt, N.T., Tang, S.L., Qi, L., 2014. Geochronology and geochemistry of the Late Triassic Longtan pluton in South China: termination of the crustal melting and Indosinian orogenesis. Int. J. Earth Sci. http://dx.doi.org/10.1007/s00531-013-0996-z.
Qiu, L., Yan, D.P., Tang, S.L., Wang, Q., Yang, W.X., Tang, X.L., Wang, J.B., 2016. Mesozoic geology of southwestern China: Indosinian foreland overthrusting and subsequent deformation. J. Asian Earth Sci. 122, 91–105.
Rao, J.R., Luo, J.L., Yi, Z.J., 1999. The mantle-crustal tectonic metallogenic model and ore-prospecting prognosis in the Xikuangshan antimony ore field. Geophys. Geochem. Explor. 23, 241–249 (In Chinese with English abstract).
Reid, A.J., Wilson, C.J.L., Shun, L., Pearson, N., Belousova, E., 2007. Mesozoic plutons of the Yidun Arc, SW China: U/Pb geochronology and Hf isotopic signature. Ore Geol. Rev. 31, 88–106.
Ren, J.S., 1991. On the geotectonics of southern China. Acta Geol. Sin. (English Edition) 4, 11–136.
Rollinson, H.R., 1993. Using Geochemical Data: Evaluation, Presentation, Interpretation. Copublished in the U.S. with J. Wiley & Sons Longman Scientific & Technical, pp. 1–352.
Shen, L.Y., Han, R.S., Li, B., Qiu, W.L., 2011. Study on the isotope geochemistry of the Maoping Pb-Zn deposit, Zhaotong, Yunnan. Mineral Resour. Geol. 25, 211–216 (in Chinese with English abstract).
Shen, N.P., Su, W.C., Fu, Y.Z., Xu, C.X., Yang, J.H., Cai, J.L., 2013. Characteristics of sulfur and lead isotopes for Banian antimony deposit in Dushan area, Guizhou Province, China: implication for origin of ore-forming materials. Acta Mineral. Sin. 33, 271–277 (in Chinese with English abstract).
Shi, M.K., Fu, B.Q., Jin, X.X., 1993. Antimony Metallogeny in Central Part of Hunan Province. Hunan Press of Science and Technology, Changsha, pp. 1–151 (in Chinese).
Shu, L.S., Zhou, X.M., Deng, P., Wang, B., Jiang, S.Y., Yu, J.H., Zhao, X.X., 2009. Mesozoic tectonic evolution of the southeast China Block: new insights from basin analysis. J. Asian Earth Sci. 34, 376–391.
Si, R.J., Gu, X.X., Pang, X.C., Fu, S.H., Li, F.Y., Zhang, M., Li, Y.H., Li, X.Y., Li, J., 2006. Geochemical character of dispersed element in sphalerite from Fule Pb-Zn polymetallic deposit, Yunnan Province. J. Mineral. Petrol. 26, 75–80 (in Chinese with English abstract).
Si, R.J., Gu, X.X., Xiao, X.C., Yu, H.T., Wang, Z.W., Chen, Y.J., Qu, N., 2011. Geochemical character of trace elements in sphalerite from Fule Pb-Zn deposit, Yunnan Province. J. Mineral. Petrol. 31, 34–40 (in Chinese with English abstract).
Song, C.A., Feng, Z.H., Lei, L.Q., 2009. Geotectonic metallogenic evolution and belt of Tin polymetal ore and exploration in Guangxi. J. Guilin Univ. Technol. 29, 207–215 (in Chinese with English abstract).
Song, X.Y., Qi, H.W., Hu, R.Z., Chen, L.M., Yu, S.Y., Zhang, J.F., 2013. Formation of thick stratiform Fe-Ti oxide layers in layered intrusion and frequent replenishment of fractionated mafic magma: evidence from the Panzhihua intrusion, SW China. Geochem. Geophys. Geosyst. 14, 712–732.
Su, W.C., Xia, B., Zhang, H.T., Zhang, X.C., Hu, R.Z., 2008. Visible gold in arsenian pyrite at the Shuiyindong Carlin-type gold deposit, Guizhou, China: implications for the environment and processes of ore formation. Ore Geol. Rev. 33, 667–679.
Su, W.C., Hu, R.Z., Xia, B., Xia, Y., Liu, Y.P., 2009a. Calcite Sm-Nd isochron age of the Shuiyindong Carlin-type gold deposit, Guizhou, China. Chem. Geol. 258, 269–274.
Su, W.C., Heinrich, C.A., Pettke, T., Zhang, X.C., Hu, R.Z., Xia, B., 2009b. Sediment-Hosted gold deposits in Guizhou, China: products of wall-rock sulfidation by deep crustal fluids. Econ. Geol. 104, 73–93.
Su, W.C., Zhang, H.T., Hu, R.Z., Ge, X., Xia, B., Chen, Y.Y., Zhu, C., 2012. Mineralogy and geochemistry of gold-bearing arsenian pyrite from the Shuiyindong Carlin-type gold deposit, Guizhou, China: implications for gold depositional processes. Mineral. Deposita 47, 653–662.
Su, W.C., Zhu, L.Y., Ge, X., Shen, N.P., Zhang, X.C., Hu, R.Z., 2015. Infrared microthermometry of fluid inclusions in stibnite from the Dachang antimony deposit, Guizhou. Acta Petrol. Sin. 31, 918–924 (in Chinese with English abstract).
Tan, Q.P., Xia, Y., Xie, Z.J., Yan, J., Wei, D.T., 2015. S, C, O, H, and Pb isotopic studies for the Shuiyindong Carlin-type gold deposit, Southwest Guizhou, China: constraints for ore genesis. Chin. J. Geochem. 93, 525–539.
Tang, J.W., Jin, J.F., Tao, Y., 1999. REE geochemical characteristics of silicified rocks of Xikuangshan antimony deposits and their geological significance. Geol.-Geochem. 27, 40–44 (in Chinese with English abstract).
Tao, Y., Gao, Z.M., Jin, J.F., Zeng, L.J., 2001. The origin of ore-forming fluid of Xikuangshan-type antimony deposits in central Hunan province. Geol.-Geochem. 1, 14–20 (in Chinese with English abstract).
Tao, Y., Gao, Z.M., Jin, J.F., Zeng, L.J., 2002. Ore-forming conditions of Xikuangshan-type antimony deposits in central Hunan. Earth Sci. 2, 184–195 (in Chinese with English abstract).
Taylor, B.E., 1986. Magmatic volatiles: Isotope variation of C, H and S. In: Stable isotopes in high temperature geological processes Reviews in Mineralogy. Mineralogist Society of American, vol. 16, pp. 185–226.
Tu, G.C., 1998. The Low Temperature Geochemistry. Science Press, Beijing (in Chinese).
Tu, G.C., 2002. Two unique mineralization areas in southwest China. Bull. Mineral., Petrol. Geochem. 21, 1–2 (in Chinese).
Wang, C.H., Wang, D.H., Liu, J.Z., Deng, Y.M., Liu, C.Q., Li, J.K., Chen, F.E., 2010. Isotope geochemical characteristics of the Shuiyindong superlarge Carlin-type gold deposit in Guizhou. Earth Sci. Front. 17, 396–403 (in Chinese with English abstract).
Wang, C.M., Deng, J., Carranza, E.J.M., Lai, X.R., 2014. Nature, diversity and temporal-spatial distributions of sediment-hosted Pb-Zn deposits in China. Ore Geol. Rev. 56, 327–351.
Wang, J.S., 2012. The metallogenesis, time and geodynamic research of low-temperature metallogenic province in southwest China (PhD thesis). Institute of geochemistry, Chinese Academy of Sciences, Guiyang, pp. 1–116 (in Chinese with English abstract).
Wang, J.S., Wen, H.J., 2015. Sm-Nd dating of hydrothermal calcites from Jiaoli-La'e mercury deposit, Guizhou Province. J. Jilin Univ.: Earth Sci. Ed. 45, 1384–1393 (in Chinese with English abstract).
Wang, M.C., Li, Z.X., Mao, Y.L., Shu, P.H., 2011. Geological features and genesis of the Laozhaiwan gold deposit in Southeastern Yunnan Province. Geol. Explor. 47, 261–267 (in Chinese with English abstract).
Wang, R., Zhang, C.Q., Wu, Y., Wei, C., 2012. The age of diabase in Tianbaoshan Pb–Zn deposit and the genetic relationship between lead–zinc mineralization and the diabase. Mineral Deposits 31, 449–450 (in Chinese).
Wang, X.C., 1992. Genesis analysis of the Tianbaoshan Pb-Zn deposit. J. Chengdu College Geol. 19, 10–20 (in Chinese with English abstract).
Wang, Y.J., Li, Z.X., 2003. History of Neoproterozoic rift basins in South China: implications for Rodinia break-up. Precambrian Res. 122, 141–158.
Wang, Y.J., Zhang, Y.H., Fan, W.M., Peng, T.P., 2005. Structural signatures and $^{40}Ar/^{39}Ar$ geochronology of the Indosinian Xuefengshan transpressive belt, South China Interior. J. Struct. Geol. 27, 985–998.
Wang, Y.J., Fan, W.M., Sun, M., Liang, X., Zhang, Y., 2007a. Geochronological, geochemical and geothermal constraints on petrogenesis of the Indosinian peraluminous granites in the South China Block: a case study in the Hunan Province. Lithos 96, 475–502.
Wang, Y.J., Fan, W.M., Cawood, P.A., Ji, S.C., Peng, T.P., Chen, X.Y., 2007b. Indosinian high-strain deformation for the Yunkaidashan tectonic belt, South China: kinematics and $^{40}Ar/^{39}Ar$ geochronological constraints. Tectonics 2007, 26. http://dx.doi.org/10.1029/2007 TC002099.
Wang, Y.J., Zhang, F.F., Fan, W.M., Zhang, G.W., Chen, S.Y., Cawood, P.A., Zhang, A.M., 2010a. Tectonic setting of the South China Block in the early Paleozoic: resolving intracontinental and ocean closure models from detrital zircon U-Pb geochronology. Tectonics 29. http://dx.doi.org/10.1029/2010TC002750.
Wang, Y.J., Zhang, A.M., Fan, W.M., Peng, T.P., Zhang, F.F., Zhang, Y.Z., Bi, X.W., 2010b. Petrogenesis of late Triassic post-collision basaltic rocks of the Langcangjiang tectonic zone, southwest China, and tectonic implication for the evolution of the eastern Paleotethys: geochronological and geochemical constrains. Lithos 120, 529–546.
Wang, Y.J., Wu, C.M., Zhang, A.M., Fan, W.M., Zhang, Y.H., Zhang, Y.Z., Peng, T.P., Yin, C.Q., 2012. Kwangsian and Indosinian reworking of the eastern South China Block: constraints on zircon U-Pb geochronology and metamorphism of amphibolite and granulite. Lithos 150, 227–242.
Wang, Y.J., Fan, W.M., Zhang, G.W., Zhang, Y.H., 2013. Phanerozoic tectonics of the South China Block: key observations and controversies. Gondwana Res. 23, 1273–1305.
Wang, Z.P., 2013. Genesis and dynamic mechanism of the epithermal ore deposits, SW Guizhou, China. A case study of gold and antimony deposits PhD thesis. Institute of Geochemistry, Chinese Academy of Sciences, Guiyang, pp. 1–150 (in Chinese with English abstract).
Wang, Z.P., Xia, Y., Song, X.Y., Liu, J.Z., Yang, C.F., Yan, B.W., 2013. Study on the evolution of ore-formation fluids for Au-Sb ore deposits and the mechanism of Au-Sb paragenesis and differentiation in the southwestern part of Guizhou Province, China. Chin. J. Geochem. 32, 56–68.
Wen, G.Z., Wu, Q., Liu, H.Y., Xie, G.Z., Lei, X.L., 1993. Preliminary study on ore controlling regularities and metallogenic mechanism of super large-sized Sb-

deposits in Xikuangshan. Geol. Explor. 7, 20–27 (in Chinese with English abstract).
Wen, H.J., Zhu, C.W., Zhang, Y.X., Cloquet, C., Fan, H.F., Fu, S.H., 2016. Zn/Cd ratios and cadmium isotope evidence for the classification of lead-zinc deposits. Sci. Reports 6. http://dx.doi.org/10.1038/srep25273.
Wu, Q.H., Cao, J., Kong, H., Shao, Y.J., Li, H., Xi, X.S., Deng, X.T., 2016. Petrogenesis and tectonic setting of the early Mesozoic Xitian granitic pluton in the middle Qin-Hang Belt, South China: Constraints from zircon U-Pb ages and bulk-rock trace element and Sr–Nd–Pb isotopic compositions. J. Asian Earth Sci. 128, 130–148.
Wu, J.C., Wang, J.R., Ou, J., Wang, S.S., Yang, S.F., Li, J.H., 2007. Inclusion-isotope geochemistry of the Baimashan-Longshan gold metallogenic belt in Hunan and its ore-forming fluid characteristics. Mineral Resour. Geol. 21, 673–678 (in Chinese with English abstract).
Wu, Y., 2013. The age and ore-forming process of MVT deposits in the boundary area of Sichuan-Yunnan-Guizhou provinces, Southwest China PhD thesis. China University of Geosciences, Beijing, pp. 1–167 (in Chinese with English abstract).
Xia, Y., 2005. Characteristics and model for Shuiyindong gold deposit in southwestern Guizhou, China PhD thesis. Institute of Geochemistry, Chinese Academy of Sciences, Guiyang, pp. 1–114 (in Chinese with English abstract).
Xia, Y., Zhang, Y., Su, W.C., Tao, Y., Zhang, X.C., Liu, J.Z., Deng, Y.M., 2009. Research on the metallogenic scale and metallogenetic prediction of the Shuiyindong superlarge Carlin-type gold deposit in Southwest Guizhou. Acta Geol. Sin. 83, 1473–1482 (in Chinese with English abstract).
Xiao, D.C., 2012. The study on ore-forming fluids in the Yata Carlin-type gold deposit, Guizhou Province Master thesis. Chengdu University of Technology, Chengdu, pp. 1–55 (in Chinese with English abstract).
Xiao, Q.M., Zeng, D.R., Jin, F.Q., Yang, M.Y., Yang, Z.F., 1992. Time-space distribution feature and exploration guide of China's Sb deposits. Geol. Prospect. 12, 9–14 (in Chinese with English abstract).
Xiao, X.G., 2014. Geochronology, ore geochemistry and genesis of the Banpo antimony deposit, Guizhou Province, China PhD thesis. Kunming University of Science and Technology, Kunming, pp. 1–138 (in Chinese with English abstract).
Xie, Q.L., Ma, D.S., Liu, Y.J., 1996. Thermal dynamic study on forming mechanism of silification-taking Xikuangshan antimony deposit as an example. Contrib. Geol. Mineral Resour. Res. 11, 1–8 (in Chinese with English abstract).
Xu, Y.G., Chung, S.L., Jahn, B.M., 2001. Petrologic and geochemical constraints on the petrogenesis of Permian-Triassic Emeishan flood basalts in southwestern China. Lithos 58, 145–168.
Xu, Z.Q., Hou, L.W., Wang, Z.X., 1992. The Orogenic Process of Songfan-Ganzi Orogenic Belt in China. Geological Publishing House, Beijing, pp. 1–190 (in Chinese with English abstract).
Yan, D.P., Zhou, M.F., Song, H.L., Wang, X.W., Malpas, J., 2003. Origin and tectonic significance of a Mesozoic multi-layer over-thrust within the Yangtze Block (South China). Tectonophysics 361, 239–254.
Yang, D.S., Shimizu, M., Shimazaki, H., Li, X.H., Xie, Q.L., 2006. Sulfur isotope geochemistry of the supergiant Xikuangshan Sb deposit, central Hunan, China: constraints on sources of ore constituents. Resour. Geol. 56, 385–396.
Yang, J.H., Cawood, P.A., Du, Y.S., Huang, H., Hu, L.S., 2012. Detrital record of Indosinian mountain building in SW China: provenance of the Middle Triassic turbidites in the Youjiang Basin. Tectonophysics 574–575, 105–117.
Yang, J.-H., Peng, J.T., Zheng, Y.F., Hu, R.Z., Bia, X.W., Zhao, J.H., Huang, J.C., Zhang, B. L., 2016. Petrogenesis of the Mesozoic Shuikoushan peraluminous I-type granodioritic intrusion in Hunan Province, South China: middle–lower crustal reworking in an extensional tectonic setting. J. Asian Earth Sci. 123, 224–242.
Yang, R.Y., Ma, D.S., Bao, Z.Y., Pan, J.Y., Cao, S.L., Xia, F., 2006. Geothermal and fluid flowing simulation of ore-forming antimony deposits in Xikuangshan. Sci. China Series (D) 8, 862–871.
Yang, S.Q., 1986. On inquiry about the genesis of Hunan stibnite ore and the direction of ore search. Hunan Geol. 5, 12–25 (in Chinese with English abstract).
Yao, J.L., Shu, L.S., Cawood, P.A., Li, J.Y., 2016. Delineating and characterizing the boundary of the Cathaysia Block and the Jiangnan orogenic belt in South China. Precambrian Res. 275, 265–277.
Yao, J., 2008. Studies on ore-forming material source and ore genesis of Laozhaiwan fine-disseminated gold deposit, in Yunnan (PhD thesis). Chengdu University of Technology, Chengdu, pp. 1–55 (in Chinese with English abstract).
Yao, Z.K., Zhu, R.B., 1993. Polygenetic compound model for the Fuzhuxi gold deposit of Hunan Province and its prospecting. Geotect. Metall. 17, 199–209 (in Chinese with English abstract).
Ye, L., Liu, T.G., Yang, Y.L., Gao, W., Pan, Z.P., Bao, T., 2014. Petrogenesis of bismuth minerals in the Dabaoshan Pb-Zn polymetallic massive sulfide deposit, northern Guangdong Province, China. J. Asian Earth Sci. 82, 1–9.
Ye, L., Nigel, J.C., Cristiana, L.C., Liu, Y.P., Zhang, Q., Liu, T.G., Gao, W., Yang, Y.L., Leonid, D., 2011. Trace and minor elements in sphalerite from base metal deposits in South China: a LA-ICPMS study. Ore Geol. Rev. 39, 188–217.
Yin, M.D., Li, W.B., Sun, X.W., 2009. Rb-Sr isotopic dating of sphalerite from the giant Huize Zn-Pb ore field, Yunnan Province, Southwestern China. Chin. J. Geochem. 28, 70–75.
Yu, J.G., 1998. Alteration features and prospecting direction in the Gutaishan gold deposit, Hunan. Hunan Geol. 3, 155–159 (in Chinese with English abstract).
Yu, J.H., Zhou, X., O'Reilly, S.Y., Zhao, L., Griffin, W.L., Wang, R., Wang, L., Chen, X., 2005. Formation history and protolith characteristics of granulite facies metamorphic rock in Central Cathaysia deduced from U-Pb and Lu–Hf isotopic studies of single zircon grains. Chin. Sci. Bull. 50, 2080–2089.
Zaw, K., Peters, S.G., Cromie, P., Burrett, C., Hou, Z.Q., 2007. Nature, diversity of deposit types and metallogenic relations of South China. Ore Geol. Rev. 31, 3–47.
Zeng, Y.F., Liu, W.J., Chen, H.D., Zheng, R.C., Zhang, J.Q., Li, X.Q., Jiang, T.C., 1995. Evolution of sedimentation and tectonics of the Youjiang composite basin, south China. Acta Geol. Sin. 69, 113–124 (in Chinese with English abstract).
Zhang, C.Q., Mao, J.W., Wu, S.P., Li, H.M., Liu, F., Guo, B.J., Gao, D.R., 2005. Distribution, characteristics and genesis of Mississippi Valley-Type lead-zinc deposits in Sichuan-Yunnan-Guizhou area. Mineral Deposits 24, 336–348 (in Chinese with English abstract).
Zhang, C.Q., Wang, D.H., Wang, Y.L., Wang, C.H., Qiu, X.P., 2012. Discuss on the metallogenic model for Gaolong gold deposit in Tianlin County, Guangxi, China. Acta Petrol. Sin. 28, 213–224 (in Chinese with English abstract).
Zhang, C.Q., Wu, Y., Wang, D.H., Chen, Y.C., Rui, Z.Y., Lou, D.B., Chen, Z.H., 2014. Brief introduction on metallogeny of Pb-Zn deposits in China. Acta Geol. Sin. 88, 2252–2268 (in Chinese with English abstract).
Zhang, C.Q., Wu, Y., Hou, L., Mao, J.W., 2015. Geodynamic setting of mineralization of Mississippi Valley-type deposits in world-class Sichuan-Yunnan-Guizhou Zn-Pb triangle, southwest China: implications from age-dating studies in the past decade and the Sm-Nd age of Jinshachang deposit. J. Asian Earth Sci. 103, 103–114.
Zhang, G.W., Guo, A.L., Wang, Y.J., Li, S.Z., Dong, Y.P., Liu, S.F., He, D.F., Cheng, S.Y., Lu, R.K., Yao, A.P., 2013. Tectonics of South China Continent and its implications. Sci. China: Earth Sci. 56, 1804–1828.
Zhang, J., Su, Q.W., Liu, X.F., He, Z.H., Zhou, Y.M., Li, Z., Zhao, K., 2014. Characteristics of geology and isotopic geochemistry of the Laozhaiwan gold deposit in southeastern Yunnan Province, China. Acta Petrol. Sin. 30, 2657–2668 (in Chinese with English abstract).
Zhang, J.W., Dai, C.G., Huang, Z.L., Luo, T.Y., Qian, Z.K., Zhang, Y., 2015. Age and petrogenesis of Anisian magnesian alkali basalts and their genetic association with the Kafang stratiform Cu deposit in the Gejiu supergiant tin-polymetallic district, SW China. Ore Geol. Rev. 69, 403–416.
Zhang, L.G., 1989. Diagenetic and Metallogenic Theory and Metallogenic Regularity. Beijing Industry University Publish House, Beijing, pp. 1–123 (in Chinese with English abstract).
Zhang, X.C., Hofstra, A., Hu, R.Z., Emsbo, P., Su, W.C., Ridley, W.I., 2005. Geochemistry and δ34S of ores and ore stage iron sulfides in Carlin-type gold deposits, Dian-Qian-Gui area, China: Implications for ore genesis. In: Mineral Deposit Research: Meeting the Global Challenge. Springer, Berlin Heidelberg, pp. 1107–1110.
Zhang, X.C., Spiro, B., Halls, C., Stanley, C.J., Yang, K.Y., 2003. Sediment-hosted disseminated gold deposits in Southwest Guizhou, PRC: their geological setting and origin in relation to mineralogical, fluid inclusion, and stable-isotope characteristics. Int. Geol. Rev. 45, 407–470.
Zhang, Y., Xia, Y., Wang, Z.P., Yan, B.W., Fu, Z.K., Chen, M., 2010. REE and stable isotope geochemical characteristics of Bojitian gold deposit, Guizhou Province. Earth Sci. Front. 17, 385–395 (in Chinese with English abstract).
Zhang, Y.M., Gu, X.X., Bai, X., Liu, R.P., Zheng, L., Wu, C.Y., Peng, Y.W., 2013. Sulfur and lead isotopic composition characteristics of the Zhesang gold deposit in Funing County, Yunnan. Earth Sci. Front. 20, 32–39 (in Chinese with English abstract).
Zhang, Y.X., Wu, Y., Tian, G., Shen, L., Zhou, Y.M., Dong, W.W., Zeng, R., Yang, X.C., Zhang, C.Q., 2014. Mineralization age and the source of ore-forming material at Lehong Pb-Zn deposit, Yunnan Province: constraints from Rb-Sr and S isotopes system. Acta Mineral. Sin. 34, 305–311 (in Chinese with English abstract).
Zhang, Z., Huang, Z.L., Zhou, J.X., Li, X.B., 2011. Sulfur isotope geochemistry of Shaojiwan Pb-Zn deposit in Northwest Guizhou, China. Acta Mineral. Sin. 31, 496–501 (in Chinese with English abstract).
Zhang, Z.B., Li, C.Y., Tu, G.C., Xia, B., Wei, Z.Q., 2006. Geotectonic evolution background and ore-forming process of Pb-Zn deposits in Chuan-Dian-Qian area of southwest China. Geotect. Metall. 30, 343–354 (in Chinese with English abstract).
Zhang, Z.L., Huang, Z.L., Rao, B., Li, W.B., Yan, Z.F., 2005a. Study on the ore-forming fluid characteristics of Huize Pb-Zn ore deposits. Contrib. Geol. Mineral Resour. Res. 20, 115–122 (in Chinese with English abstract).
Zhang, Z.L., Huang, Z.L., Rao, B., Guan, T., Yan, Z.F., 2005b. Concentration mechanism of ore-forming fluid in Huize lead-zinc deposits, Yunnan Province. Earth Sci.-J. China Univ. Geosci. 30, 443–450 (in Chinese with English abstract).
Zhao, J.G., 2001. Geological characteristics of Au deposit and its prospecting foreground at Daping gold mine, Hongjiang. Hunan Geol. 20, 171–176 (in Chinese with English abstract).
Zhao, J.L., Qiu, J.S., Liu, L., Wang, r.Q., 2015. Geochronological, geochemical and Nd–Hf isotopic constraints on the petrogenesis of Late Cretaceous A-type granites from the southeastern coast of Fujian Province, South China. J. Asian Earth Sci. 105, 338–359.
Zhao, J.H., Zhou, M.F., Yan, D.P., Zheng, J.P., Li, J.W., 2011. Reappraisal of the ages of Neoproterozoic strata in South China: no connection with the Grenvillian orogeny. Geology 39, 299–302.
Zheng, C.L., 1992. Study on ore-controlling structures of Pb-Zn ore region in Northwestern Guizhou Province. Mineral Resour. Geol. 6, 193–200 (in Chinese with English abstract).
Zheng, M.H., Wang, X.C., 1991. Genesis of the Daliangzi Pb-Zn Deposit in Sichuan, China. Econ. Geol. 86, 831–846.
Zhong, H., Campbell, I.H., Zhu, W.G., Allen, C.M., Hu, R.Z., Xie, L.W., He, D.F., 2011a. Timing and source constraints on the relationship between mafic and felsic intrusions in the Emeishan large igneous province. Geochim. Cosmochim. Acta 75, 1374–1395.
Zhong, H., Qi, L., Hu, R.Z., Zhou, M.F., Gou, T.Z., Zhu, W.G., Liu, B.G., Chu, Z.Y., 2011b. Rhenium-osmium isotope and platinum-group elements in the Xinjie layered

intrusion, SW China: Implications for source mantle composition, mantle evolution, PGE fractionation and mineralization. Geochim. Cosmochim. Acta 75, 1621–1641.
Zhou, C.X., Wei, C.S., Guo, J.Y., Li, C.Y., 2001. The source of metals in the Qilinchang Zn-Pb deposit, Northeastern Yunnan, China: Pb-Sr isotope constraints. Econ. Geol. 96, 583–598.
Zhou, J.C., Wang, X.L., Qiu, J.S., 2009. Geochronology of Neoproterozoic mafic rocks and sandstones from northeastern Guizhou, South China: coeval arc magmatism and sedimentation. Precambrian Res. 170, 27–42.
Zhou, J.X., Huang, Z.L., Bao, G.P., 2013a. Geological and sulfur-lead-strontium isotopic studies of the Shaojiwan Pb-Zn deposit, southwest China: implications for the origin of hydrothermal fluids. J. Geochem. Explor. 128, 51–61.
Zhou, J.X., Huang, Z.L., Yan, Z.F., 2013b. The origin of the Maozu carbonate-hosted Pb-Zn deposit, southwest China: constrained by C-O-S-Pb isotopic compositions and Sm-Nd isotopic age. J. Asian Earth Sci. 73, 39–47.
Zhou, J.X., Huang, Z.L., Zhou, M.F., Li, X.B., Jin, Z.G., 2013c. Constraints of C-O-S-Pb isotope compositions and Rb-Sr isotopic age on the origin of the Tianqiao carbonate-hosted Pb-Zn deposit, SW China. Ore Geol. Rev. 53, 77–92.
Zhou, J.X., Huang, Z.L., Zhou, M.F., Zhu, X.K., Muchez, P., 2014. Zinc, sulfur and lead isotopic variations in carbonate-hosted Pb–Zn sulfide deposits, southwest China. Ore Geol. Rev. 58, 41–54.
Zhou, J.X., Bai, J.H., Huang, Z.L., Zhu, D., Yan, Z.F., Lv, Z.C., 2015. Geology, isotope geochemistry and geochronology of the Jinshachang carbonate-hosted Pb-Zn deposit, southwest China. J. Asian Earth Sci. 98, 272–284.
Zhou, J.X., Luo, K., Li, B., Huang, Z.L., Yan, Z.F., 2016. Geological and isotopic constraints on the origin of the Anle carbonate-hosted Zn-Pb deposit in northwestern Yunnan Province, SW China. Ore Geol. Rev. 74, 88–100.
Zhou, M.F., Yan, D.P., Kennedy, A.K., Li, Y.Q., Ding, J., 2002. SHRIMP zircon geochronological and geochemical evidence for Neoproterozoic arc-related magmatism along the western margin of the Yangtze Block, South China. Earth Planet. Sci. Lett. 196, 51–67.
Zhou, M.F., Zhao, J.H., Qi, L., 2006. Zircon U-Pb geochronology and elemental and Sr-Nd isotopic geochemistry of Permian mafic rocks in the Funing area, SW China. Contrib. Mineral. Petrol. 151, 1–19.
Zhou, M.-F., Zhao, X.-F., Chen, W.T., Li, X.C., Wang, W., Yan, D.Y., Qiu, H.N., 2014. Proterozoic Fe–Cu metallogeny and supercontinental cycles of the southwestern Yangtze Block, southern China and northern Vietnam. Earth Sci. Rev. 139, 59–82.
Zhou, X.M., Sun, T., Shen, W., Shu, L., Niu, Y., 2006. Petrogenesis of Mesozoic granitoids and volcanic rocks in south China, a response to tectonic evolution. Episodes 29, 26–33.
Zhou, Y.F., 1993. The application of regional gravity to the deep geology and mineralization prognosis in Guangxi. Geol. Guangxi 6, 15–24 (in Chinese with English abstract).
Zhu, C.W., Wen, H.J., Zhang, Y.X., Fan, H.F., Fu, S.H., Xu, J., Qin, T.R., 2013. Characteristics of Cd isotopic compositions and their genetic significance in the lead-zinc deposits of SW China. Sci. China-Earth Sci. 56, 2056–2065.